

1 **The effect of emission source chemical profiles on simulated PM<sub>2.5</sub> components:**  
2 **sensitivity analysis with CMAQv5.0.2**

3 Zhongwei Luo<sup>a,b,1</sup>, Yan Han<sup>a,b,c,1</sup>, Kun Hua<sup>a,b</sup>, Yufen Zhang<sup>a,b\*</sup>, Jianhui Wu<sup>a,b</sup>, Xiaohui  
4 Bi<sup>a,b</sup>, Qili Dai<sup>a,b</sup>, Baoshuang Liu<sup>a,b</sup>, Yang Chen<sup>c</sup>, Xin Long<sup>c</sup>, Yinchang Feng<sup>a,b\*</sup>

5 <sup>a</sup>State Environmental Protection Key Laboratory of Urban Ambient Air Particulate  
6 Matter Pollution Prevention and Control & Tianjin Key Laboratory of Urban  
7 Transport Emission Research, College of Environmental Science and Engineering,  
8 Nankai University, Tianjin 300350, China.

9 <sup>b</sup>CMA-NKU Cooperative Laboratory for Atmospheric Environment-Health Research,  
10 Tianjin 300350, China.

11 <sup>c</sup>Research Center for Atmospheric Environment, Chongqing Institute of Green and  
12 Intelligent Technology, Chinese Academy of Sciences, Chongqing 400714, China.

13

14

15 \*Corresponding authors:

16 Y. F. Zhang (zhafox@nankai.edu.cn). And Y. C. Feng (fengyc@nankai.edu.cn).

17

18 <sup>1</sup>Z. W. Luo and Y. Han equally contribute to this work

19 **Abstract**

20 The chemical transport model (CTM) is an essential tool for air quality prediction  
21 and management, widely used in air pollution control and health risk assessment.  
22 However, the current models do not perform very well in reproducing the observations  
23 of some major chemical components, for example, sulfate, nitrate, ammonium and  
24 organic carbon. Studies suggested that the uncertainties of model chemical mechanism,  
25 source emission inventory and meteorological field can cause inaccurate simulation  
26 results. Still, the emission source profile (used to create speciated emission inventories  
27 for CTMs) of PM<sub>2.5</sub> has not been fully taken into account in current numerical  
28 simulation. ~~This study aims to answer (1) Whether the variation of source profile  
29 adopted in CTMs has an impact on the simulation of PM<sub>2.5</sub> chemical components? (2)  
30 How much does it impact? (3) How does the impact work?~~ Based on the characteristics  
31 and variation rules of chemical components in typical PM<sub>2.5</sub> sources, different  
32 simulation scenarios were designed and the sensitivity of simulated PM<sub>2.5</sub> components  
33 to source chemical profile was explored. Our findings showed that the influence of  
34 source profile changes on simulated PM<sub>2.5</sub> components' concentrations could not be  
35 ignored. Simulation results of some components were sensitive to the adopted source  
36 profile in CTMs. Moreover, there was a linkage effect, the variation of some  
37 components in the source profile would bring changes to the simulated results of other  
38 components. These influences are connected to chemical mechanisms of the model  
39 since the variation of species allocations in emission sources can affect potential  
40 composition and phase state of aerosols, chemical reaction priority and multicomponent  
41 chemical balance in thermodynamic equilibrium system. We also found that the  
42 perturbation of ~~the~~ PM<sub>2.5</sub> source profile caused the variation of simulated gaseous  
43 pollutants, which indirectly indicated that the perturbation of source profile would  
44 affect the simulation of secondary PM<sub>2.5</sub> components. Our paper highlights the  
45 necessity that the representativeness and timeliness of the source profile should be paid  
46 enough attention when using CTMs for simulation. ~~Given the vital role of air quality~~

47 ~~simulation in environment management and health risk assessment, the~~  
48 ~~representativeness and timeliness of source profile should be considered.~~

49 **Keywords**

50 PM<sub>2.5</sub>; source profile; component; numerical simulation; chemical transport model

51 **1. Introduction**

52 Ambient fine particulate matter (PM<sub>2.5</sub>) pollution in some key regions of China  
53 has attracted much attention (Liang et al., 2020; Huang et al., 2021). The chemical  
54 components of PM<sub>2.5</sub>, including elements (Al, Si, Fe, Mn, Ti, Cu, Zn, Pb, etc.), water-  
55 soluble ions (SO<sub>4</sub><sup>2-</sup>, NO<sub>3</sub><sup>-</sup>, Cl<sup>-</sup>, F<sup>-</sup>, NH<sub>4</sub><sup>+</sup>, Na<sup>+</sup>, K<sup>+</sup>, Mg<sup>2+</sup>, Ca<sup>2+</sup>, etc.), and carbon-  
56 containing components (Organic Carbon, OC; Elemental Carbon, EC) (Yang et al.,  
57 2011; Li et al., 2013), have different physical and chemical properties, such as reactivity,  
58 thermal stability, particle size distribution, residence time, optical properties, health  
59 hazards, etc (Seinfeld and Pandis, 2006; Tang et al., 2006). According to long-term  
60 monitoring results, in most regions of China, SO<sub>4</sub><sup>2-</sup>, NO<sub>3</sub><sup>-</sup>, NH<sub>4</sub><sup>+</sup> and OC are the most  
61 important species in ambient PM<sub>2.5</sub> (Li et al., 2017a; Li et al., 2021), which has a certain  
62 adverse impact on human health (Shi et al., 2018) and ecosystem, such as acid rain in  
63 southwest China (Han et al., 2019), food security (Zhou et al., 2018), etc.

64 The chemical transport models (CTMs) play an important role in policy making  
65 for regulatory purposes. Based on the scientific understanding of atmospheric physical  
66 and chemical processes, CTMs are built to simulate the transport, reaction and removal  
67 of pollutants on a certain scale in horizontal and vertical directions. With the  
68 development of CTMs, the simulation accuracy of PM<sub>2.5</sub> concentration has been  
69 significantly improved. Higher requirements have been put forward for the precise  
70 simulation of PM<sub>2.5</sub> components so as to provide support for the use of CTMs in human  
71 health risk assessment, climate effects, pollution sources apportionment, and so on  
72 (Peterson et al., 2020; Lv et al., 2021). However, the current models perform not very  
73 well in simulating some components (for example, PM<sub>2.5</sub>-bound sulfate, nitrate,  
74 ammonium, trace elements, etc.) (Zheng et al., 2015; Fu et al., 2016; Ying et al., 2018;  
75 Cao et al., 2021). In the current literatures, the correlation coefficient (R) and  
76 normalized mean bias (NMB) are highly variable and inconsistent between the  
77 simulated and the observed values (listed in Table S1). This is mainly attributable to the  
78 uncertainties of model chemical mechanism, source emission inventory and

79 meteorological field simulation.

80 The chemical mechanisms involved in CTMs are derived from parameterized  
81 assumptions based on laboratory simulation and field observations. The actual  
82 atmospheric chemical processes are very complex, and some reaction mechanisms are  
83 still limitedly understood. In addition, the integration of chemical reactions and  
84 simplified treatment methods in the model cannot fully reflect the correlation among  
85 atmospheric pollutants. For example, in some model mechanisms, important sulfate and  
86 nitrate formation pathways through new heterogeneous chemistry were added,  
87 including the chemical reaction between SO<sub>2</sub> and aerosol, NO<sub>2</sub>/NO<sub>3</sub>/N<sub>2</sub>O<sub>3</sub> and aerosol  
88 (Zheng et al., 2015), nitrous acid oxidized SO<sub>2</sub> to produce sulfate (Zheng et al., 2020),  
89 dust particles promoted the oxidation of SO<sub>2</sub> (Yu et al., 2020), modified the uptake  
90 coefficients for heterogeneous oxidation of SO<sub>2</sub> to sulfate (Zhang et al., 2019), updated  
91 the heterogeneous N<sub>2</sub>O<sub>5</sub> parameterization (Foley et al., 2010). Even though the  
92 aforementioned processes can significantly improve the simulation of SO<sub>4</sub><sup>2-</sup> and NO<sub>3</sub><sup>-</sup>,  
93 there is still a gap between the modeled and the actual atmospheric chemical processes.

94 The uncertainty of meteorological field simulation is another crucial reason for the  
95 simulation deviation, especially on heavy pollution days, the variation trends of PM<sub>2.5</sub>  
96 chemical components were not well-captured (Ying et al., 2018; Qi et al., 2019; Wang  
97 et al., 2022). Precipitation is the key meteorological factor determining wet removal of  
98 pollutants; boundary layer height and wind speed are the main factors affecting  
99 convection and transport of pollutants; solar radiation, temperature and relative  
100 humidity are the key factors affecting the formation of secondary particles (Huang et  
101 al., 2019; Chen et al., 2020). Some literature reported that deviation from precipitation  
102 and wind field simulation might lead to underestimation of SO<sub>4</sub><sup>2-</sup>, NO<sub>3</sub><sup>-</sup> and NH<sub>4</sub><sup>+</sup>  
103 (Cheng et al., 2015; Zhang et al., 2017). Devaluation of liquid water path and cloud  
104 cover cause a decrease of sulfate formation in cloud, and ultimately results in  
105 significantly underestimated components in simulation values (Sha et al., 2019; Foley  
106 et al., 2010). Underestimation of temperature and relative humidity may also cause  
107 adverse effects of temperature- and/or relative humidity-dependence chemical reaction

108 in the simulation (Sha et al., 2019).

109 The uncertainty of source emission inventory also significantly affects the  
110 simulation results of PM<sub>2.5</sub> components (Shi et al., 2017; Sha et al., 2019). Due to  
111 incomplete information or insufficient representativeness, pollutant emissions are  
112 sometimes overestimated or underestimated, and the method for temporal and spatial  
113 allocation also needs to be improved.

114 In particular, the emission source profile of PM<sub>2.5</sub> (Hereinafter referred to as  
115 "source profile"), used to create speciated emission inventories for CTMs (Hsu et al.,  
116 2019), has not been fully taken into account in the current numerical simulation. In the  
117 reported literatures, PM<sub>2.5</sub> species allocation coefficients of emission sources are  
118 commonly treated in the following ways: (1) allocated PM<sub>2.5</sub> components of source  
119 emissions by referring to source profile data in published literature or database like the  
120 US SPECIATE (Fu et al., 2013; Wang et al., 2014; Ying et al., 2018); (2) chemical  
121 profiles come from local measurement (Fu et al., 2013; Appel et al., 2013). However,  
122 with the development of production technology and the innovation of pollution  
123 treatment technology in recent years, some source profiles have changed dramatically  
124 (Bi et al., 2019), such as SO<sub>4</sub><sup>2-</sup> from coal burning, ~~SO<sub>4</sub><sup>2-</sup>~~its content in PM<sub>2.5</sub> is generally  
125 low in coal-fired power plant without desulfurizing facilities, while existing coal-fired  
126 power plants using limestone/gypsum wet desulphurization, the contents of SO<sub>4</sub><sup>2-</sup> in  
127 PM<sub>2.5</sub> are significantly higher than that without desulfurization facilities (Zhang et al.,  
128 2020). The timeliness of PM<sub>2.5</sub> species allocation coefficients in current CTMs also  
129 needs to be considered.

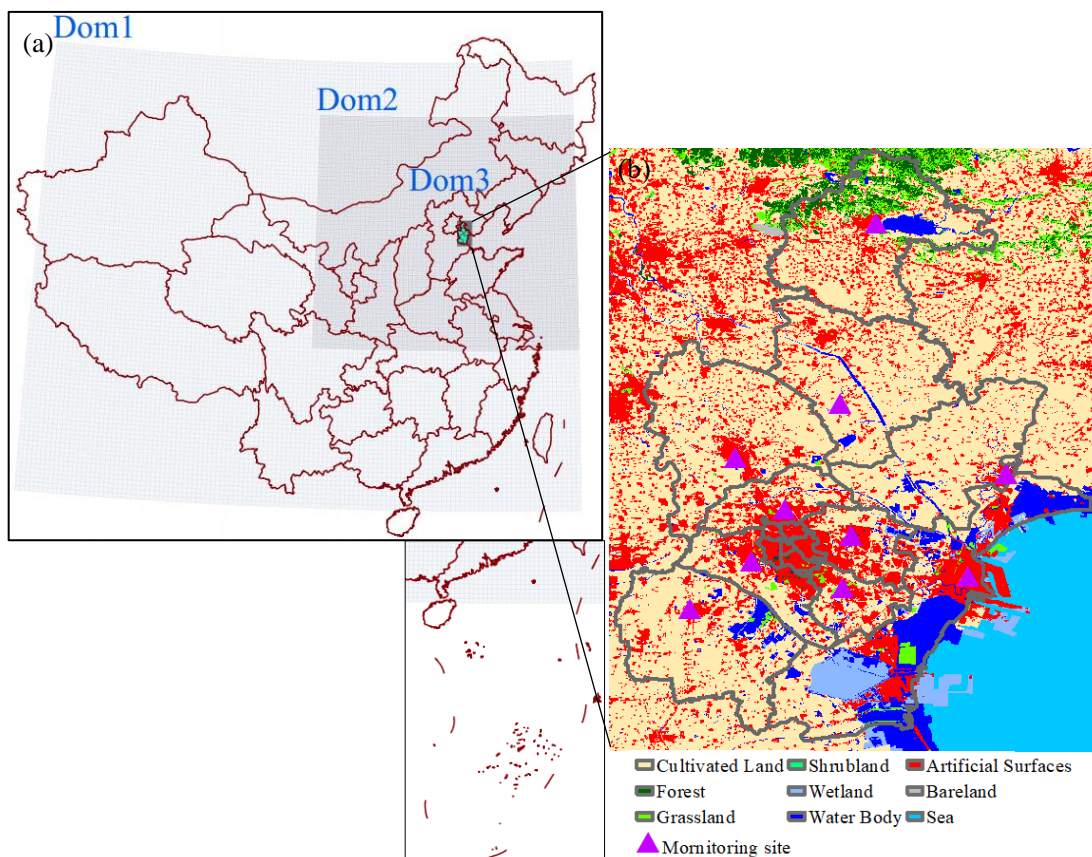
130 This paper attempts to answer the following questions: (1) Whether the variation  
131 of the source profile adopted in the model has an impact on the simulated results of  
132 PM<sub>2.5</sub> chemical components? (2) How much does it impact? (3) How does the impact  
133 work? Aiming at these problems above, chemical composition and its variation law for  
134 typical PM<sub>2.5</sub> emission sources are summarized, on this basis, sensitivity tests are  
135 designed to identify whether PM<sub>2.5</sub> source profiles and species allocation in the model  
136 are important parameters that affect the simulation results of chemical components?

137 concentrations in PM<sub>2.5</sub>. We take CMAQ (one of the most widely used CTMs), MEIC  
138 (a high-resolution inventory of anthropogenic air pollutants in China) as the carriers.  
139 The same kind of experiment is also applicable to other CTMs and emission inventories.  
140 The aim of this study is to provide support for the effective utilization of source profiles  
141 in the CTMs and improvement of the simulation schemes.

## 142 **2. Model and Data**

### 143 **2.1 Model configuration**

144 Weather Research and Forecasting model (WRF-3.7.1), the widely used  
145 Community Multiscale Air Quality model (CMAQv5.0.2) (Eder and Yu, 2006; Yu et al.,  
146 2014), and Multi-resolution Emission Inventory for China (MEICv1.3) have been used  
147 in this study. MEIC-, developed by Tsinghua University, mainly tracked anthropogenic  
148 emissions in China including coal-fired power plants, industry, vehicles, residents and  
149 agriculture ([http://meicmodel.org/?page\\_id=135](http://meicmodel.org/?page_id=135)) (Li et al., 2017b; Zheng et al., 2018).  
150 The WRF model was used to generate meteorological inputs for the CMAQ model.  
151 Three nested modeling domains consisting of 36 km×36 km (Dom1), 12 km×12km  
152 (Dom2), and 4 km×4km (Dom3) horizontal grid sizes were set, as shown in Fig. 1. The  
153 initial and boundary conditions for WRF were based on the North American Regional  
154 Reanalysis data archived at National Center for Atmospheric Research (NCAR). In  
155 addition, surface and upper air observations obtained from NCAR were used to further  
156 refine the analysis data. The modeling was conducted from Oct. 1 to Oct.30 in 2018,  
157 and major configurations we used in CMAQ were illuminated as follows: Gas-phase  
158 chemistry was based on the CB05 mechanism and the aerosol dynamics/chemistry was  
159 based on the aero6 module (cb05tucl\_ae6\_aq). The detailed model configurations were  
160 shown in Table S2, and regional distribution of PM<sub>2.5</sub> emission sources were shown in  
161 Figure S1.



162  
 163 Fig.1 Modeling domains of the CMAQ model. (a) The three-domain nested CMAQ domains; (b)  
 164 Land use and observation sites of Dom3 (Data source of Land use: GLOBELAND30,  
 165 www.globeland30.org, National Geomatics Center of China).

## 166 2.2 Selection and comparison of PM<sub>2.5</sub> emission source profile

167 The PM<sub>2.5</sub> emission source profiles from database of Source Profiles of Air  
 168 Pollution (SPAP) (<http://www.nkspap.com:9091/>), U.S. Environmental Protection  
 169 Agency's (EPA) SPECIATE database ([https://www.epa.gov/air-emissions-](https://www.epa.gov/air-emissions-modeling/speciate)  
 170 [modeling/speciate](https://www.epa.gov/air-emissions-modeling/speciate)) as well as from published literature were selected, respectively. The  
 171 SPAP was developed by the State Environment Protection Key Laboratory of Urban  
 172 Particulate Air Pollution Prevention, Nankai University, China. This database contains  
 173 more than 3000 size-resolved source profiles of stationary combustion sources,  
 174 industrial processes, vehicle exhaust, biomass burning, dust and other sources, collected  
 175 from more than 40 cities in China since 2001. In addition to inorganic elements, water-  
 176 soluble ions, OC, EC and other conventional components, some source profiles also  
 177 encompass a series of tracer information, such as organic markers, isotopes, single  
 178 particle mass spectrometry, VOCs and other gaseous precursors. Based on species in



179 the aerosol chemical mechanism (AERO6) of CMAQ (Appel et al., 2013; Chapel Hill,  
 180 2012), we selected 15 components in PM<sub>2.5</sub> source profiles including Al, Ca, Cl, EC,  
 181 Fe, K, Mg, Mn, Na, OC, Si, Ti, NH<sub>4</sub><sup>+</sup>, NO<sub>3</sub><sup>-</sup> and SO<sub>4</sub><sup>2-</sup>, the remaining components are  
 182 classified as “other”. In the database of Source Profiles of Air Pollution (SPAP) and  
 183 U.S. Environmental Protection Agency’s (EPA) SPECIATE database, these four source  
 184 categories (coal-fired power plant, industry process, transportation sector and  
 185 residential coal combustion) contain a series of sub-categories. But the MEIC emission  
 186 inventory does not include the corresponding sub-categories. So we take the average  
 187 values of source profiles in each source category as representing source profile, the  
 188 details could also be seen in our previous work (Bi et al., 2019); Then multiply  
 189 inventory emissions by profile fraction to get emissions of specific chemical  
 190 components.

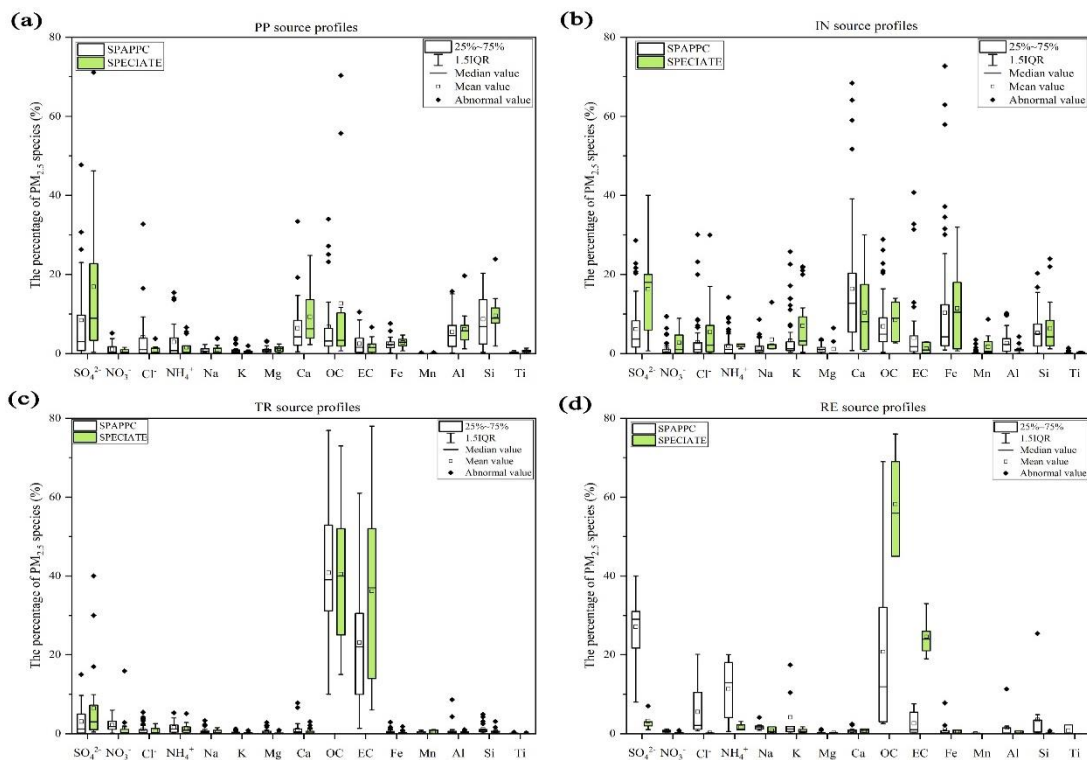
191 To determine the similarity between the two groups of source profiles, Coefficient  
 192 Divergence (CD) is calculated using the following formula (Wongphatarakul et al.,  
 193 1998):

$$194 \quad CD_{jk} = \sqrt{\frac{1}{p} \sum_{i=1}^p \left( \frac{x_{ij} - x_{ik}}{x_{ij} + x_{ik}} \right)^2} \dots\dots\dots (1)$$

195 Where CD<sub>jk</sub> is the coefficient of divergence of source profile *j* and *k*, *p* is the  
 196 number of chemical components in source profile, *x<sub>ij</sub>* is the weight percentage for  
 197 chemical component *i* in source profile *j*, *x<sub>ik</sub>* is the weight percentage for *i* in source  
 198 profile *k* (%). The CD value is in the range of 0 to 1, if the two source profiles are  
 199 similar, the value of CD is close to 0; if the two are very different, the value is close to  
 200 1.

201 **Coal-fired power plant (PP).** Coal-fired power plants remain the main coal  
 202 consumers in China, which accounted for 50.2% of total coal consumption in 2019  
 203 (NBS, 2021) and gained much more attention, especially with the wide implementation  
 204 of the ultralow emission standards, PM<sub>2.5</sub> emission characteristics have changed  
 205 accordingly (Wu et al., 2020; Wu et al., 2022). There are obvious differences in PM<sub>2.5</sub>  
 206 source profiles between SPAPPC (SPAP database and published source profiles in

207 China) and SPECIATE (U.S.EPA SPECIATE database), the CD value of these two  
 208 groups lie between 0.34 and 0.92 ( $0.64\pm 0.10$ ), detailed information is shown in Table  
 209 S3 and Figure S2. The percentages of species in PP source profiles are plotted in Fig.  
 210 2(a). The main components in SPAPPC are sorted by Si,  $\text{SO}_4^{2-}$ , OC, Ca with average  
 211 values of  $8.7\pm 6.8\%$ ,  $8.5\pm 11.5\%$ ,  $6.8\pm 9.1\%$  and  $6.5\pm 6.9\%$ , respectively; The SPECIATE  
 212 are enriched in  $\text{SO}_4^{2-}$  ( $16.9\%\pm 20.0\%$ ), OC ( $12.7\%\pm 21.8\%$ ), Si ( $9.6\pm 5.0\%$ ) and Ca  
 213 ( $9.3\pm 7.3\%$ ), higher than SPAPPC. Coal properties, burning conditions, pollution control  
 214 measures and emission sampling methods are the main reasons for those great  
 215 percentage fluctuations. Different treatment processes of flue gases, e.g. wet/dry  
 216 limestone, ammonia and double-alkali flue gas desulfurization, will affect the  
 217 percentages of components in source profiles (Zhang et al., 2020). It has been reported  
 218 that the percentage of Ca, Mg,  $\text{SO}_4^{2-}$  and  $\text{Cl}^-$  in PP profiles increased after the limestone-  
 219 gypsum method was used in coal-fired power plants (Bi et al., 2019). Besides that, the  
 220 percentage of  $\text{Cl}^-$  in SPAPPC is obviously higher than that in SPECIATE, which might  
 221 attribute to the generally higher  $\text{Cl}^-$  content in raw coal in China (Guo et al., 2004).



222  
 223  
 224

Fig. 2 Chemical profiles for  $\text{PM}_{2.5}$  emitted from (a) coal-fired power plants (PP), (b) industry processes (IN), (c) transportation sector (TR), (d) residential coal combustion (RE). Data obtained

225 from SPAPPC (SPAP database and published source profiles in China) and SPECIATE (U.S. EPA  
226 SPECIATE database)

227 **Industrial process(IN).** Industrial emissions are one of the major sources of PM<sub>2.5</sub>  
228 (Hopke et al., 2020), the percentages of Ca, Fe, OC and SO<sub>4</sub><sup>2-</sup> are relatively high both  
229 in SPAPPC and SPECIATE, but the shares in different source profile database varied,  
230 their CD values vary from 0.45 to 0.94 (0.72±0.09) (Detailed information were shown  
231 in Table S4~S7 and Figure S3). In SPAPPC, these four components account for  
232 16.4±14.9%, 10.4±14.4%, 6.9±6.1%, 6.2±6.4%, the proportions in SPECIATE are  
233 10.4±9.8%, 11.4±10.6%, 8.5±4.9%, 16.3±13.3%, respectively (Fig. 2(b)). Large  
234 variations of components and their percentages in industrial processes are attributed to  
235 the manufacturing processes, raw material, pollution control measures and so on (Ji et  
236 al., 2017; Bi et al., 2019; Gao et al., 2022). For example, Ca, Al, OC and SO<sub>4</sub><sup>2-</sup> are found  
237 to have the highest percentage in cement sources (Guo et al., 2021); Fe, Si and SO<sub>4</sub><sup>2-</sup>  
238 are the most abundant species in steel industry emission (Guo et al., 2017).

239 **Transportation sector (TR).** Traffic contributed a large fraction of PM<sub>2.5</sub> in many  
240 locations (Hopke et al., 2022). It is well-known that the transportation sector makes a  
241 dominant contribution of OC and EC. The main components of PM<sub>2.5</sub> emitted from  
242 traffic sources are OC, EC and SO<sub>4</sub><sup>2-</sup> both in SPAPPC and SPECIATE, but still vary in  
243 wide range, their CD values fall between 0.33 and 0.86 (0.69±0.09) (Detailed  
244 information was given in Table S8~S10 and Figure S4). In SPAPPC, the percentages of  
245 OC, EC and SO<sub>4</sub><sup>2-</sup> are 40.8±15.0%, 23.1±13.8%, 3.1±3.7%, and in SPECIATE, the  
246 percentages are 40.6±16.4%, 36.1±21.5%, 6.4±9.9%, respectively (Fig. 2(c)). These  
247 significant differences mainly attribute to the vehicle type, fuel quality, mixing ratio  
248 between oil and gas and the combustion phase in vehicle engine and so on (Xia et al.,  
249 2017).

250 **Residential coal combustion (RE).** Residential coal combustion, as the leading  
251 source of global PM<sub>2.5</sub> emission (Weagle et al., 2018), has a much higher emission  
252 factor than coal-fired power plant (Wu et al., 2022). The fraction of components vary  
253 greatly in the profiles measured from SPAPPC and SPECIATE, their CD values are  
254 0.75±0.10 (Detailed information was given in Table S11 and Figure S5), SO<sub>4</sub><sup>2-</sup>, OC,

255  $\text{NH}_4^+$  and EC make the main contribution to  $\text{PM}_{2.5}$  emitted from residential coal  
256 combustion. In SPAPPC, the average percentages of  $\text{SO}_4^{2-}$ , OC,  $\text{NH}_4^+$ , EC are  
257  $27.1\pm 10.1\%$ ,  $20.7\pm 20.6\%$ ,  $11.3\pm 7.7\%$ ,  $2.6\pm 2.8\%$ , respectively. In SPECIATE, the  
258 average percentages are OC ( $58.2\pm 14.0\%$ ), EC ( $24.6\pm 5.4\%$ ),  $\text{SO}_4^{2-}$  ( $3.2\pm 2.3\%$ ) and  
259  $\text{NH}_4^+$  ( $1.6\pm 1.0\%$ ) (Fig. 2(d)). Total percentages of OC and EC in SPECIATE are over  
260 80%, obviously higher than that in SPAPPC, while a higher percentage of  $\text{SO}_4^{2-}$ , Cl<sup>-</sup>, K  
261 and Si are observed in SPAPPC. The coal type and properties, burning condition are the  
262 main factors affecting the percentages of  $\text{PM}_{2.5}$  components, like the chunk coal burning  
263 has relatively higher percentages of OC, EC,  $\text{SO}_4^{2-}$ ,  $\text{NO}_3^-$  and  $\text{NH}_4^+$  than honeycomb  
264 briquette (Wu et al., 2021; Song et al., 2021).

265 Briefly, many factors can affect  $\text{PM}_{2.5}$  source profiles, and with the innovation of  
266 manufacturing technique and pollution control technology, changes in fuel and raw and  
267 auxiliary materials, the main chemical components and their percentages would change  
268 dramatically. To explore whether the variations of source profile adopted in CMAQ  
269 model would be one of the important factors affecting the simulated  $\text{PM}_{2.5}$  component,  
270 we designed a series of simulation tests to address the following issues.

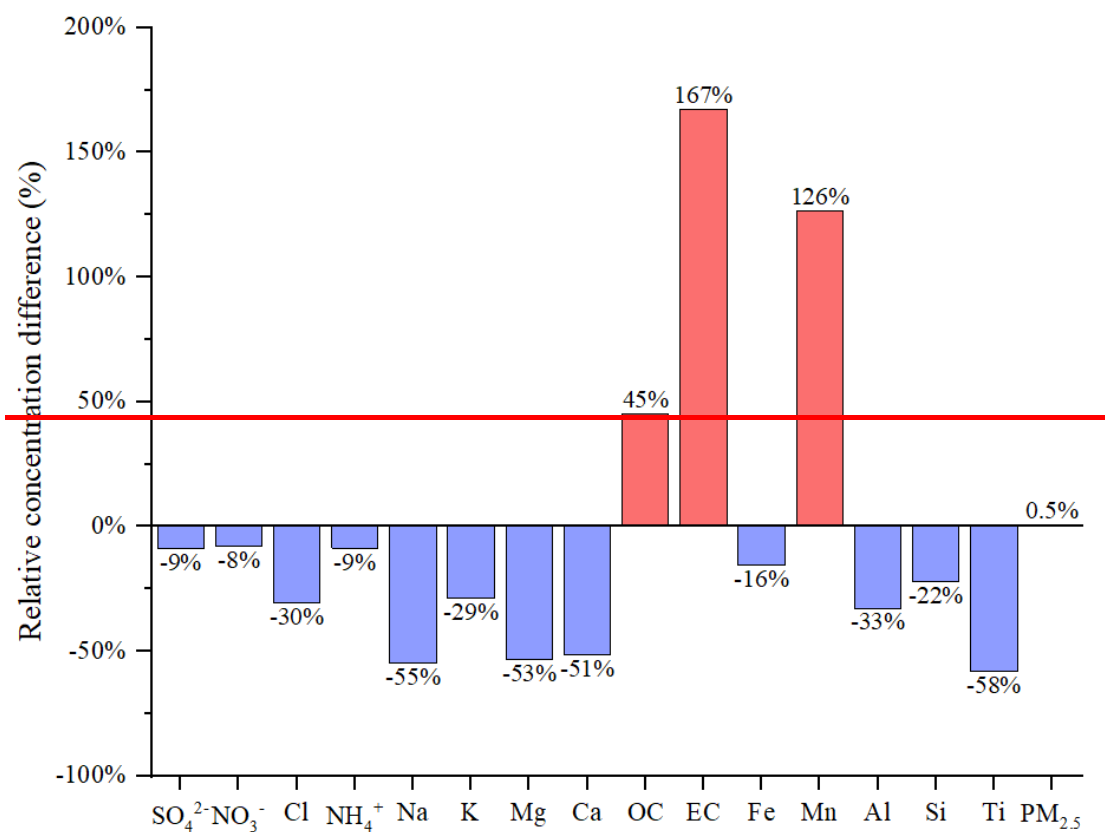
### 271 **3 Is there an impact of variation of source profile on the simulation results?**

272 In this part, we separately selected source profiles from SPAPPC and SPECIATE  
273 databases and applied them in emission inventory for simulating  $\text{PM}_{2.5}$  and its  
274 components with other modeling conditions unchanged, corresponding to case  
275 CMAQ\_SPA and CMAQ\_SPE. The detailed information of source profiles ~~is~~ were  
276 shown in Figure S6.

277 By comparing the selected SPAPPC source profiles with the selected SPECIATE  
278 source profiles, the coefficient divergences for the four main source categories were  
279  $\text{CD}_{\text{PP}}(0.67) > \text{CD}_{\text{RE}}(0.62) > \text{CD}_{\text{TR}}(0.60) > \text{CD}_{\text{IN}}(0.60)$ , which meant the selected source  
280 profiles in the two simulation cases were quite different. The average simulated  
281 concentration of  $\text{PM}_{2.5}$  and its components at each ambient air quality monitoring  
282 station (Table S12) were extracted from CMAQ outputs. We selected one air quality

283 monitoring station (Site 8 as the selected station here and any site could be available)  
 284 to explore the effect of emission source chemical profiles on simulated PM<sub>2.5</sub>  
 285 components, then used the left 9 sites to further illustrate the conclusions suggested.

286 The simulation results for PM<sub>2.5</sub> species under CMAQ\_SPA and CMAQ\_SPE  
 287 cases also showed big differences (as shown in Fig. 3 and Table S13). The largest  
 288 difference in average simulated concentration was EC with CAMQ\_SPE giving higher  
 289 by 167% than CMAQ\_SPA; For OC and Mn, higher values were also given by  
 290 CMAQ\_SPE than by CMAQ\_SPA (45% and 126% on average, respectively); For the  
 291 other components of concern, the simulated concentration by CMAQ\_SPE was lower  
 292 than CMAQ\_SPA with Ti (58%), Na (55%), Mg (53%), Ca (51%), Al (33%), Cl  
 293 (30%), K (29%), Si (22%), Fe (16%), NH<sub>4</sub><sup>+</sup> (9%), SO<sub>4</sub><sup>2-</sup> (9%), NO<sub>3</sub><sup>-</sup> (8%), separately.  
 294 While the simulated PM<sub>2.5</sub> concentrations under the two cases were quite close. The  
 295 influence of source profile variation on the simulated PM<sub>2.5</sub> concentration was not  
 296 significant, but the influence on the simulation of chemical components in PM<sub>2.5</sub> could  
 297 not be ignored.



298

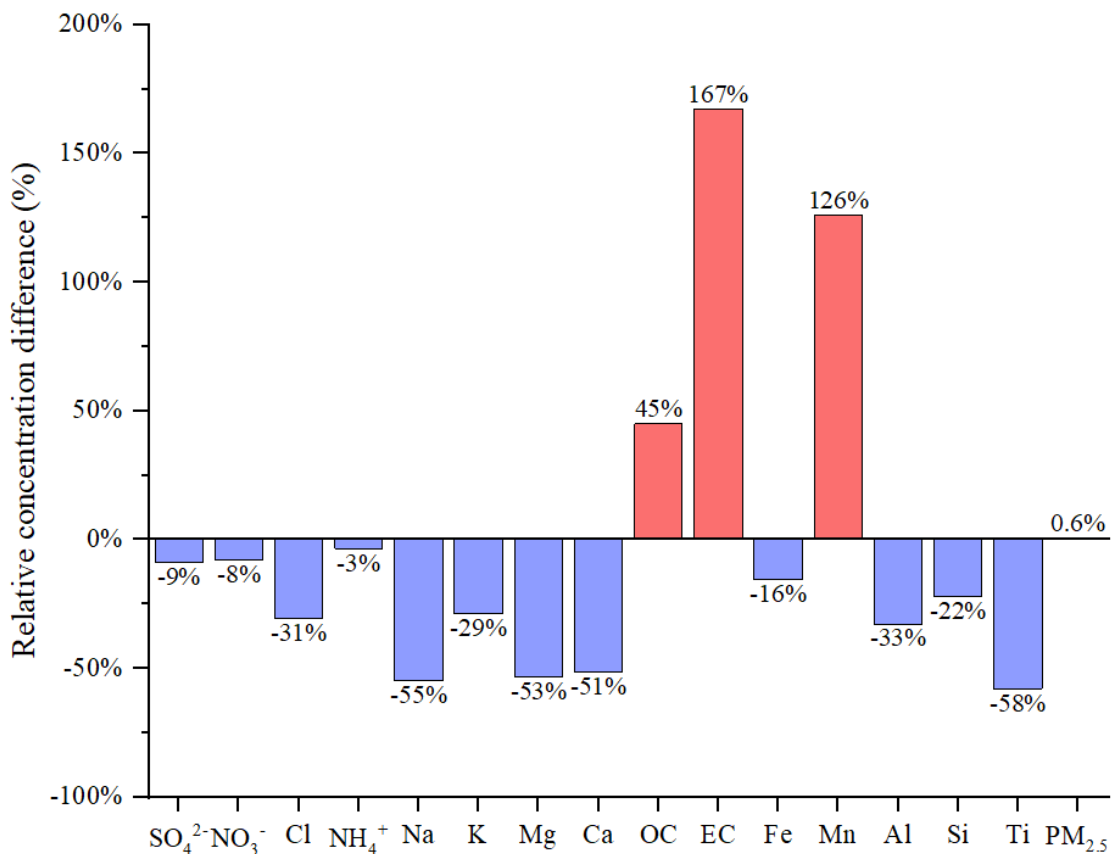
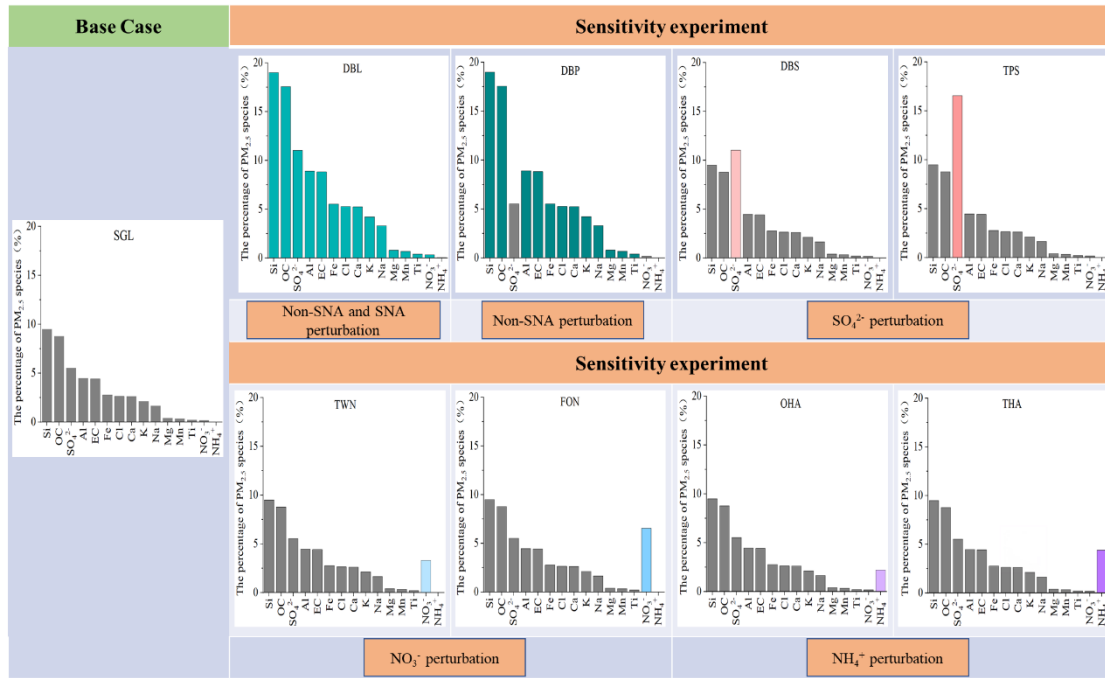


Fig. 3 The relative concentration difference of average simulated results (PM<sub>2.5</sub> and its components) between CMAQ\_SPE and CAMQ\_SPA (relative to CAMQ\_SPA) during simulation period; PM<sub>2.5</sub> source profiles from SPAPPC and SPECIATE database were used to create speciated emission inventories for CMAQ, corresponding to case CMAQ\_SPA and CMAQ\_SPE, respectively.

#### 4 How much does it impact?

To quantitatively characterize how much the source profiles affect the simulation results, we selected the chemical composition of code 000002.5 (Variety of different categories, used for the overall average composite profiles (Hsu et al., 2019) in the US EPA Speciate\_5.0\_0 database for species allocation of PM<sub>2.5</sub> components. The corresponding percentages of EC, OC, Mn, Fe, Ti, Al, Si, Ca, Mg, K, Na, Cl, NH<sub>4</sub><sup>+</sup>, NO<sub>3</sub><sup>-</sup> and SO<sub>4</sub><sup>2-</sup> in PM<sub>2.5</sub> were shown in Fig. 4 (SGL, base case simulation).



311

312

313

314

Fig. 4 The general roadmap of sensitivity tests (The histogram in each case were the speciation profile in CTMs; SNA represent<sup>ed</sup>  $\text{SO}_4^{2-}$ ,  $\text{NO}_3^-$ , and  $\text{NH}_4^+$ , Non-SNA represent<sup>ed</sup> other components in  $\text{PM}_{2.5}$ ).

315

Table 1 The content of sensitivity experiment cases

Experiment Cases	Description <sup>3</sup>
Case DBL: add perturbation to Non-SNA and SNA <sup>1</sup>	The percentage of all the listed components in the source profile of base case (SGL) were doubled, and the proportion of unlisted components (Other) <sup>2</sup> decreased to 9%.
Case DBP: add perturbation to Non-SNA	The percentages of non-SNA were doubled and SNA( $\text{SO}_4^{2-}$ , $\text{NO}_3^-$ , $\text{NH}_4^+$ ) species stayed the same with that in SGL (the cumulative percentage of listed species was 85.3%), the proportion of unlisted components decreased to 14.7%.
Case DBS and TPS: add perturbation to $\text{SO}_4^{2-}$	The percentage of $\text{SO}_4^{2-}$ was doubled (11%, DBS, represented Double Sulfate), tripled (16.5%, TPS, represented Triple Sulfate) and the other listed 14 species stayed the same with that in SGL (the cumulative percentage of listed species was 51% and 57%, respectively), the proportion of unlisted components decreased to 49% and 43%.
Case TWN and FON: add perturbation to $\text{NO}_3^-$	The $\text{NO}_3^-$ content was raised up to 20 times (3.3%, TWN) and 40 times (6.6%, FON) of that in SGL (0.16%), the other 14 species stayed the same with SGL (the cumulative percentage of listed species was 48.6% and 51.9%, respectively), the proportion of unlisted components decreased to 51.4% and 48.1%.

Case OHA and THA:  
add perturbation to  $\text{NH}_4^+$

The  $\text{NH}_4^+$  content was raised up to 100 times (2.2%, OHA), 200 times (4.4%, THA) of that in SGL (0.02%), the other 14 species stayed the same with SGL (the cumulative percentage of listed species was 47.7% and 49.9%, respectively), the proportion of unlisted components decreased to 52.3% and 50.1%.

Note:

1. SNA represented  $\text{SO}_4^{2-}$ ,  $\text{NO}_3^-$ , and  $\text{NH}_4^+$ , Non-SNA represented other components in  $\text{PM}_{2.5}$ .
2. The listed components contained Al, Ca, Cl, EC, Fe, K, Mg, Mn, Na, OC, Si, Ti,  $\text{NH}_4^+$ ,  $\text{NO}_3^-$  and  $\text{SO}_4^{2-}$ , unlisted components ~~are~~ were classified as Other.
3. The source profiles in all cases listed in the table were calculated based on the base case SGL. In the design of simulation cases, the reason why the disturbance amplitude of  $\text{NH}_4^+$  and  $\text{NO}_3^-$  were significantly higher than that of other components such as  $\text{SO}_4^{2-}$  and Non-SNA, was because the percentages of  $\text{NH}_4^+$  and  $\text{NO}_3^-$  in the base source profile (SGL, based on the chemical composition of code 000002.5 in the EPA Speciate\_5.0\_0 database ) were very low, while the percentage of  $\text{NH}_4^+$  and  $\text{NO}_3^-$  in SPAPPC exhibited in section 2.2 were orders of magnitude higher than those in SGL.

316        Given the large number and complex chemical composition of  $\text{PM}_{2.5}$ , it ~~is~~ was  
317        advisable to classify them reasonably before designing sensitivity experiments. The  
318        Case DBL was to double the percentage of the listed 15 components mentioned in the  
319        above base case(SGL) (the details are shown in Fig. 4 and Table 1). As the percentage  
320        of these components increased, the proportion of unlisted components (represented by  
321        “Other”) decreased to 9% in order to meet the requirement that the total percentage of  
322        all components is 100%. Then we compared the simulation results before (SGL case)  
323        and after perturbation (DBL case) in species allocation of  $\text{PM}_{2.5}$  sources.

324        In the case DBL, when the percentage of all the components except “other” were  
325        doubled in the source profile, the simulated concentrations of Al, Ca, Cl, EC, Fe, K,  
326        Mg, Mn, Na, OC, Si and Ti doubled as well, while the simulated concentration of  $\text{NO}_3^-$   
327        and  $\text{SO}_4^{2-}$  increased at about 3%, 10% and  $\text{NH}_4^+$  decreased by 4%, respectively,  
328        although the simulated concentration of  $\text{PM}_{2.5}$  was not obviously changed (Detailed  
329        simulation results were shown in Table S14). The simulation test results for SNA ( $\text{SO}_4^{2-}$ ,  
330         $\text{NO}_3^-$ , and  $\text{NH}_4^+$ ) and Non-SNA were obviously different. Therefore, we divided the  
331        components in the source profile into two groups (Non-SNA and SNA) and designed a  
332        series of sensitivity tests listed in next section to further explore how species allocation  
333        of  $\text{PM}_{2.5}$  in emission sources affect the simulation results. The sketch of sensitivity



334 experiment design idea ~~is~~was shown in Figure S7.

#### 335 4.1 Sensitivity tests design

336 Sensitivity tests were designed by changing the percentages of the target  
337 components and related components in the base case (SGL): add perturbation on each  
338 component of Non-SNA, on  $\text{SO}_4^{2-}$ , on  $\text{NO}_3^-$ , and on  $\text{NH}_4^+$ . The general roadmap of  
339 sensitivity tests ~~is~~was shown in Fig. 4, and the illustration of each case was summarized  
340 in Table 1. The basic rules must be followed: a) perturbation on the percentage of each  
341 component in source profile fell within the variation range of its measured value  
342 described in section 2.2. b) The sum of the percentage of listed Non-SNA, SNA and  
343 Other components in  $\text{PM}_{2.5}$  source profile was 100%.

#### 344 4.2 Sensitivity of simulated components to changes in source profile

345 We proposed the sensitivity coefficient ( $\delta$ ) as evaluation index. The calculation  
346 formula is as follows:

$$347 \delta_{i,p} = \frac{\frac{C_{i\_case}}{C_{PM_{2.5\_case}}} \times 100\% - \frac{C_{i\_base}}{C_{PM_{2.5\_base}}} \times 100\%}{P_{p\_case} - P_{p\_base}} \quad (\text{For DBL and DBP, } p = i; \text{For other cases, } p = j)$$

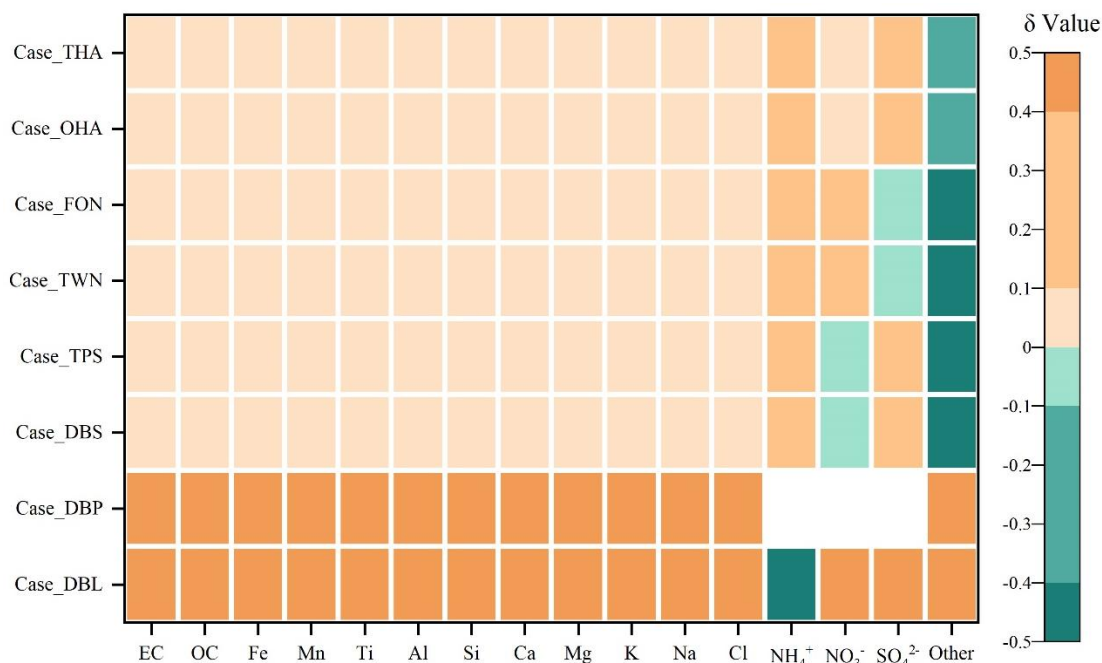
348 ..... (2)

349 Wherein,  $\delta_{i,p}$  is the sensitivity coefficient of component  $i$  relative to component  $p$ ,  
350 representing the change in simulated value of its content in ambient  $\text{PM}_{2.5}$  corresponded  
351 to 1% perturbation in the source profiles.  $C_{i\_case}$  is the simulated  
352 concentrationsimulation result of component  $i$  in each sensitivity experiment case,  
353  $\mu\text{g}/\text{m}^3$ ;  $C_{i\_base}$  is the simulated concentrationsimulation result of components  $i$  in base  
354 case,  $\mu\text{g}/\text{m}^3$ ;  $C_{PM_{2.5\_case}}$  is the simulated concentrationsimulation result of  $\text{PM}_{2.5}$  in each  
355 sensitivity experiment case,  $\mu\text{g}/\text{m}^3$ ;  $C_{PM_{2.5\_base}}$  is the simulated concentrationsimulation  
356 result of  $\text{PM}_{2.5}$  in base case,  $\mu\text{g}/\text{m}^3$ ;  $P_{p\_case}$  is the percentage of component  $p$  in source  
357 profile of sensitivity experiment case, %;  $j$  is the perturbed component  $j$  in different  
358 source profile of sensitivity experiment cases;  $P_{p\_base}$  is the percentage of component  $p$   
359 in source profile of base case, %.

360 The positive value of  $\delta$  means the simulated concentration of  $\text{PM}_{2.5}$  component

361 increases (decreases) with the increase (decrease) of perturbation on the percentage of  
362 components in source profile, negative  $\delta$  is just the opposite. If the absolute value of  $\delta$   
363 is less than or equal to 0.1, the simulated component is considered to be insensitive to  
364 the corresponding variation of source profile; If the absolute value of  $\delta$  falls between  
365 0.1 and 0.4 (included), the simulated component is considered to be sensitive to the  
366 variation of source profile; If the absolute value of  $\delta$  is larger than 0.4, the simulated  
367 component is very sensitive to the variation of source profile. The greater the absolute  
368 value of  $\delta$  is, indicates the variation of source profile adopted in CMAQ has more  
369 obvious impact on the simulated results of PM<sub>2.5</sub> chemical components.

370 Fig.5 listed the sensitivity coefficients of simulated ambient PM<sub>2.5</sub> components to  
371 the perturbation of source profile under each test case. In case DBL (doubled the  
372 percentage of the listed components in the source profile of base case and decreased the  
373 proportion of unlisted other components to 9%), the sensitivity coefficient ( $\delta$ ) of NH<sub>4</sub><sup>+</sup>  
374 was negative, and the absolute value was high, indicating that the simulated proportion  
375 of NH<sub>4</sub><sup>+</sup> in ambient PM<sub>2.5</sub> decreased, and it was very sensitive to the variation of source  
376 profile. Conversely, the sensitivity coefficient of NO<sub>3</sub><sup>-</sup> was close to 1, which illustrated  
377 that the simulated proportion of NO<sub>3</sub><sup>-</sup> in ambient PM<sub>2.5</sub> increased proportionally with  
378 the change in source profile. The simulated SO<sub>4</sub><sup>2-</sup> also showed a very sensitive property.  
379 The simulated Non-SNA concentrations were doubled when compared to the base case  
380 (SGL).



381  
 382 Fig. 5 The sensitivity coefficients ( $\delta$ ) of simulated components to the perturbation of adopted source profile in different cases. Note: Each small color box in the figure represented the sensitivity level  
 383 (indicated by the legend on the right) of PM<sub>2.5</sub> components (the x-coordinate) in different cases (y-  
 384 coordinate). The blank grids in DBP case indicated no perturbation to SNA in PM<sub>2.5</sub> source profile  
 385 under this case.  
 386

387 In case DBP, when the percentages of listed Non-SNA (Al, Ca, Cl, EC, Fe, K, Mg,  
 388 Mn, Na, OC, Si and Ti) in the source profile were doubled, the simulated proportions  
 389 of Non-SNA in ambient PM<sub>2.5</sub> synchronous increased, and were very sensitive to the  
 390 change in the adopted source profile with a sensitivity coefficient ( $\delta$ ) of 0.5.  
 391 Interestingly, the simulated concentration of SNA in ambient PM<sub>2.5</sub> also changed  
 392 although the SNA in source profile did not change, the concentration of NO<sub>3</sub><sup>-</sup> and SO<sub>4</sub><sup>2-</sup>  
 393 increased by 2% and 3%, respectively, NH<sub>4</sub><sup>+</sup> decreased by 10% (Detail simulation  
 394 results of each case were shown on Table S15~S21).

395 Under SO<sub>4</sub><sup>2-</sup> perturbation cases (Case DBS and Case TPS), we found the simulated  
 396 results of Non-SNA and NO<sub>3</sub><sup>-</sup> had no obvious variation compared with the base case.  
 397 Either in Case DBS or in Case TPS, the  $\delta$  of Non-SNA and NO<sub>3</sub><sup>-</sup> were between -0.1 to  
 398 0.1. But when the percentage of SO<sub>4</sub><sup>2-</sup> was doubled in source profile (DBS), the  
 399 simulated concentration of NH<sub>4</sub><sup>+</sup> and SO<sub>4</sub><sup>2-</sup> increased by 6% and 8%, respectively. In  
 400 Case TPS (the percentage of SO<sub>4</sub><sup>2-</sup> was tripled), the simulated concentration of NH<sub>4</sub><sup>+</sup>

401 and  $\text{SO}_4^{2-}$  were increased by 11% and 16%, respectively. The  $\delta$  of  $\text{NH}_4^+$  and  $\text{SO}_4^{2-}$  were  
402 0.12 and 0.36, sensitive toward to positive direction with the increase of  $\text{SO}_4^{2-}$  in the  
403 source profile.

404 In the situation of  $\text{NO}_3^-$  perturbation in source profile (Case TWN and Case FON),  
405 the simulated Non-SNA hardly change when compared to the base case, while changing  
406 patterns of simulated SNA were different. The simulation concentration of  $\text{NH}_4^+$   
407 increased by 2.6% and 5.4% compared with the base case, the simulated  $\text{NO}_3^-$  increased  
408 by 14% and 30%, the simulated  $\text{SO}_4^{2-}$  decreased slightly, even could be neglected in  
409 some observation sites. The simulated concentrations of Non-SNA and  $\text{SO}_4^{2-}$  were  
410 insensitive to the perturbation of  $\text{NO}_3^-$  in source profile;  $\text{NH}_4^+$  was sensitive, and  $\text{NO}_3^-$   
411 was very sensitive.

412 When we put perturbation on  $\text{NH}_4^+$  in the source profile (Case OHA and Case  
413 THA), the simulation results of Non-SNA were almost not changed, the simulated  
414 concentration of  $\text{SO}_4^{2-}$ ,  $\text{NH}_4^+$ ,  $\text{NO}_3^-$  increased. The  $\delta$  of SNA to the variation of  $\text{NH}_4^+$  in  
415 the source profile were positive and  $\delta_{\text{SO}_4^{2-}, \text{NH}_4^+} > \delta_{\text{NH}_4^+, \text{NH}_4^+} > \delta_{\text{NO}_3^-, \text{NH}_4^+}$ ,  $\text{SO}_4^{2-}$  and  $\text{NH}_4^+$   
416 were sensitive to the  $\text{NH}_4^+$  perturbation in the source profile, but  $\text{NO}_3^-$  was not so  
417 sensitive.

418 In general, the simulation results of components in ambient  $\text{PM}_{2.5}$  were affected in  
419 one way or another by the change of source profiles adopted by CMAQ. Both of the  
420 simulated Non-SNA and SNA were very sensitive to the perturbation of Non-SNA in  
421 source profile. When the percentage of SNA changed in the source profile, simulated  
422 Non-SNA generally have little change, but the simulation results of SNA could change  
423 in different patterns: the simulated  $\text{SO}_4^{2-}$  was very sensitive and  $\text{NH}_4^+$  was sensitive to  
424 the perturbation of  $\text{SO}_4^{2-}$  in source profile; simulated  $\text{NO}_3^-$  was very sensitive and  $\text{NH}_4^+$   
425 was sensitive to the perturbation of  $\text{NO}_3^-$  in source profile;  $\text{SO}_4^{2-}$  and  $\text{NH}_4^+$  were  
426 sensitive to the perturbation of  $\text{NH}_4^+$  in source profile. The simulated component such  
427 as  $\text{SO}_4^{2-}$  was influenced not only by the change of  $\text{SO}_4^{2-}$  itself but also by other  
428 components like some Non-SNA and  $\text{NH}_4^+$  in the source profile. In other words, there  
429 was a linkage effect, variation of some components in the source profile would bring

430 changes to the simulated results of other components.

### 431 **5 How does the impact work?**

432 The variation of species allocation in emission sources can directly affect the  
433 composition of aerosol system in CTMs. In CMAQv5.0.2, the aerosol thermodynamic  
434 equilibrium process is carried out according to ISORROPIA II, including a  $\text{SO}_4^{2-}$ - $\text{NO}_3^-$   
435 - $\text{Cl}^-$ - $\text{NH}_4^+$ - $\text{Na}^+$ - $\text{K}^+$ - $\text{Mg}^{2+}$ - $\text{Ca}^{2+}$ - $\text{H}_2\text{O}$  system (Detailed equilibrium relations were shown  
436 in Table S22). Some assumptions ~~had~~have been made in the ISORROPIA model to  
437 simplify the simulation system (Fountoukis and Nenes, 2007): (1) Because the vapor  
438 pressure of sulfuric acid and metal salts (such as  $\text{Na}^+$ ,  $\text{Ca}^{2+}$ ,  $\text{K}^+$ ,  $\text{Mg}^{2+}$ ) ~~were~~are very  
439 low, it ~~was~~is assumed that all the sulfuric acid and metal salts in the system existed in  
440 the aerosol phase; (2) For ammonia in the system, it ~~was~~is preferred to have an  
441 irreversible reaction with sulfuric acid to produce ammonium sulfate. Only when there  
442 ~~was~~is still surplus  $\text{NH}_3$  after the neutralization of  $\text{H}_2\text{SO}_4$ , can it have a reversible  
443 reaction with  $\text{HNO}_3$  and  $\text{HCl}$  to produce  $\text{NH}_4\text{NO}_3$  and  $\text{NH}_4\text{Cl}$ . (3) For sulfuric acid in  
444 the system, if there ~~were~~are metal ions (such as  $\text{Ca}^{2+}$ ,  $\text{Mg}^{2+}$ ,  $\text{K}^+$ ,  $\text{Na}^+$ ) in the system,  
445 sulfuric acid would react with metal ions to produce metal salts. Only in the case of  
446 insufficient sodium, sulfuric acid would react with ammonia. Based on these  
447 assumptions, the ISORROPIA model ~~introduceed~~introduces the following three  
448 judgment parameters ( $R_1$ ,  $R_2$  and  $R_3$ -) to determine the simulation subsystems, these  
449 parameters are calculated by the following formulas:

450 
$$R_1 = \frac{[\text{NH}_4^+] + [\text{Ca}^{2+}] + [\text{K}^+] + [\text{Mg}^{2+}] + [\text{Na}^+]}{[\text{SO}_4^{2-}]} \dots\dots\dots (3)$$

451 
$$R_2 = \frac{[\text{Ca}^{2+}] + [\text{K}^+] + [\text{Mg}^{2+}] + [\text{Na}^+]}{[\text{SO}_4^{2-}]} \dots\dots\dots (4)$$

452 
$$R_3 = \frac{[\text{Ca}^{2+}] + [\text{K}^+] + [\text{Mg}^{2+}]}{[\text{SO}_4^{2-}]} \dots\dots\dots (5)$$

453 Where  $[X]$  denotes molar concentration of component ( $\text{mol}\cdot\text{m}^{-3}$ ),  $R_1$ ,  $R_2$  and  $R_3$   
454 are termed as “total sulfate ratio”, “crustal species and sodium ratio” and “crustal

455 species ratio” respectively; The number of species and equilibrium reactions are  
456 determined by the relative abundance of NH<sub>3</sub>, Na, Ca, K, Mg, HNO<sub>3</sub>, HCl, H<sub>2</sub>SO<sub>4</sub>, as  
457 well as the ambient relative humidity and temperature. Guided by the value of R<sub>1</sub>, R<sub>2</sub>  
458 and R<sub>3</sub>, 5 aerosol composition regimes in ISORROPIA are defined. (Detail rules are  
459 shown in Table S27 and solving procedure in Figure S8). R<sub>1</sub>, R<sub>2</sub> and R<sub>3</sub> under each  
460 sensitivity test case were shown in Fig. 6. These components achieved thermodynamic  
461 equilibrium in the order of preference for more stable salts, obviously, the simulation  
462 processes of these components may influence each other.

### 463 5.1 General results

464 Our sensitivity experiment focuses on examining the impact of source profile  
465 changes on simulated PM<sub>2.5</sub> components. For given meteorological conditions, we  
466 analyze the sensitivity of simulated components to variations in the source chemical  
467 profile by comparing the simulation results between perturbed cases and base case. In  
468 this paper, R<sub>1</sub>, R<sub>2</sub>, R<sub>3</sub> and the potential aerosol species under each sensitivity test case  
469 were shown in Table 2. These components achieved thermodynamic equilibrium in the  
470 order of preference for more stable salts, obviously, the simulation processes of these  
471 components may influence each other.

472 -

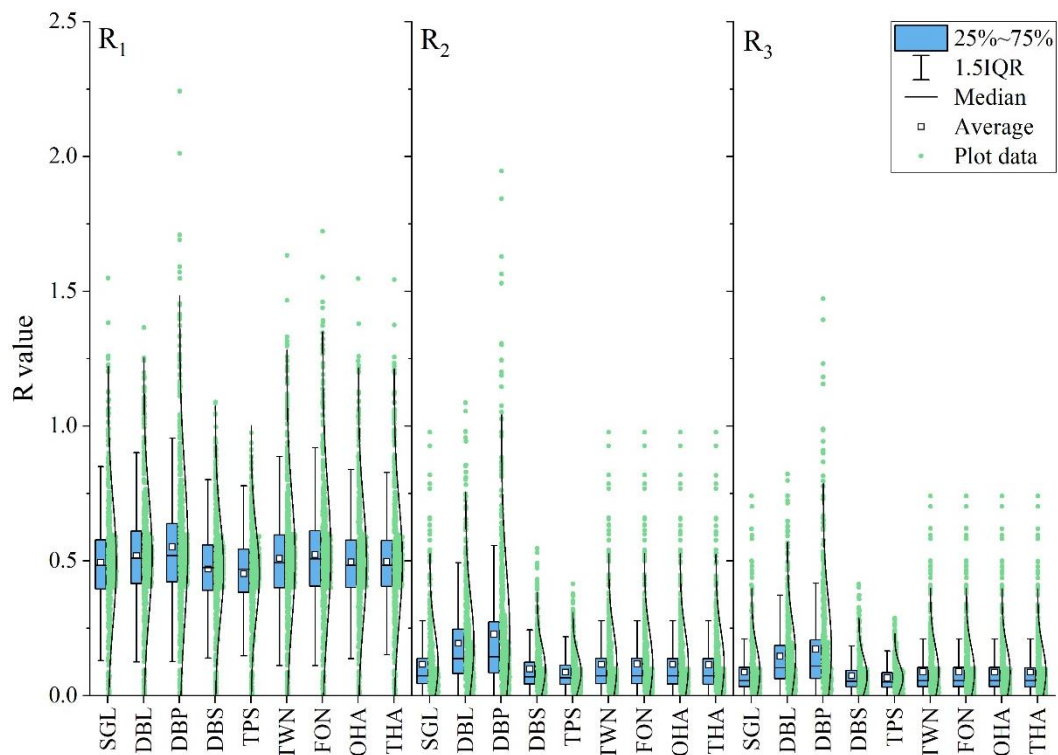


Fig. 6 R values' distribution of among base case and different sensitivity test cases

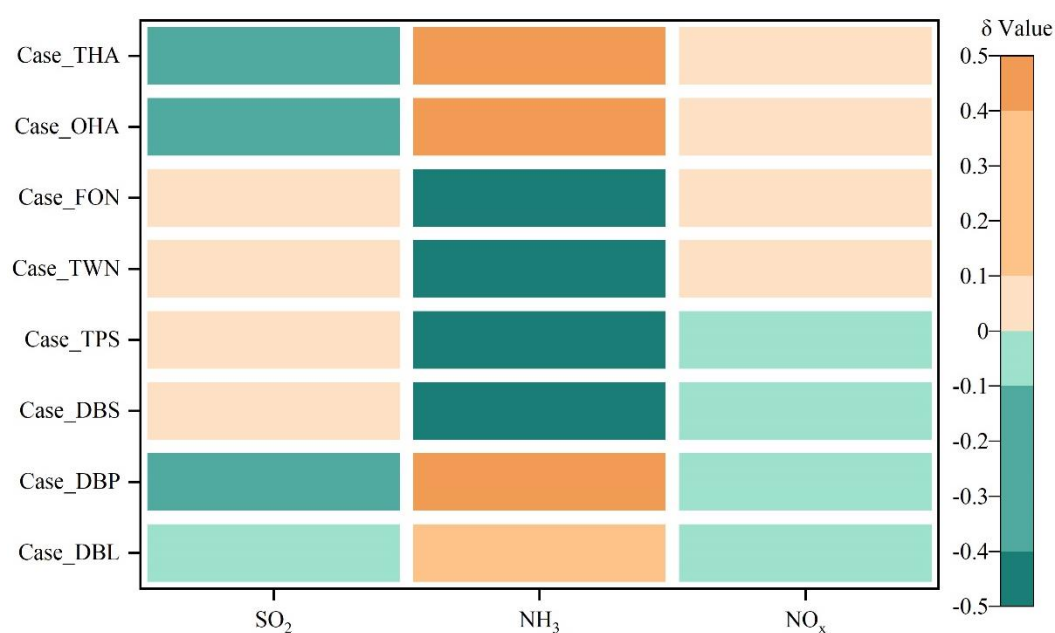
Table 2 Potential aerosol species in ISORROPIA II under different cases

Cases	R <sub>1</sub>	R <sub>2</sub>	R <sub>3</sub>	Solid phase species*
SGL	2.53	2.52	1.9	CaSO <sub>4</sub> , MgSO <sub>4</sub> , K <sub>2</sub> SO <sub>4</sub> , Na <sub>2</sub> SO <sub>4</sub> , NaCl, NaNO <sub>3</sub> , NH <sub>4</sub> Cl, NH <sub>4</sub> NO <sub>3</sub>
DBL	2.53	2.52	1.9	CaSO <sub>4</sub> , MgSO <sub>4</sub> , K <sub>2</sub> SO <sub>4</sub> , Na <sub>2</sub> SO <sub>4</sub> , NaCl, NaNO <sub>3</sub> , NH <sub>4</sub> Cl, NH <sub>4</sub> NO <sub>3</sub>
DBP	5.04	5.03	3.79	CaSO <sub>4</sub> , MgSO <sub>4</sub> , K <sub>2</sub> SO <sub>4</sub> , CaCl <sub>2</sub> , Ca(NO <sub>3</sub> ) <sub>2</sub> , MgCl <sub>2</sub> , Mg(NO <sub>3</sub> ) <sub>2</sub> , KCl, KNO <sub>3</sub> , NaCl, NaNO <sub>3</sub> , NH <sub>4</sub> Cl, NH <sub>4</sub> NO <sub>3</sub>
DBS	1.26	1.26	0.95	CaSO <sub>4</sub> , MgSO <sub>4</sub> , K <sub>2</sub> SO <sub>4</sub> , KHSO <sub>4</sub> , Na <sub>2</sub> SO <sub>4</sub> , NaHSO <sub>4</sub> , (NH <sub>4</sub> ) <sub>2</sub> SO <sub>4</sub> , NH <sub>4</sub> HSO <sub>4</sub> , (NH <sub>4</sub> ) <sub>3</sub> H(SO <sub>4</sub> ) <sub>2</sub>
TPS	0.84	0.84	0.63	CaSO <sub>4</sub> , KHSO <sub>4</sub> , NaHSO <sub>4</sub> , NH <sub>4</sub> HSO <sub>4</sub>
TWN	2.53	2.52	1.9	CaSO <sub>4</sub> , MgSO <sub>4</sub> , K <sub>2</sub> SO <sub>4</sub> , Na <sub>2</sub> SO <sub>4</sub> , NaCl, NaNO <sub>3</sub> , NH <sub>4</sub> Cl, NH <sub>4</sub> NO <sub>3</sub>
FON	2.53	2.52	1.9	CaSO <sub>4</sub> , MgSO <sub>4</sub> , K <sub>2</sub> SO <sub>4</sub> , Na <sub>2</sub> SO <sub>4</sub> , NaCl, NaNO <sub>3</sub> , NH <sub>4</sub> Cl, NH <sub>4</sub> NO <sub>3</sub>
OHA	3.58	2.52	2.95	CaSO <sub>4</sub> , MgSO <sub>4</sub> , K <sub>2</sub> SO <sub>4</sub> , CaCl <sub>2</sub> , Ca(NO <sub>3</sub> ) <sub>2</sub> , MgCl <sub>2</sub> , Mg(NO <sub>3</sub> ) <sub>2</sub> , KCl, KNO <sub>3</sub> , NaCl, NaNO <sub>3</sub> , NH <sub>4</sub> Cl, NH <sub>4</sub> NO <sub>3</sub>
THA	4.64	2.52	4.02	CaSO <sub>4</sub> , MgSO <sub>4</sub> , K <sub>2</sub> SO <sub>4</sub> , CaCl <sub>2</sub> , Ca(NO <sub>3</sub> ) <sub>2</sub> , MgCl <sub>2</sub> , Mg(NO <sub>3</sub> ) <sub>2</sub> , KCl, KNO <sub>3</sub> , NaCl, NaNO <sub>3</sub> , NH <sub>4</sub> Cl, NH <sub>4</sub> NO <sub>3</sub>



476 \*The solid phase species were determined based on the research of (Fountoukis and Nenes, 2007)

477 In Non-SNA perturbation case, when the percentage of Non-SNA in source profile  
478 doubled (Case DBP), meant there were more Na, K, Mg, Ca, Cl participated in aerosol  
479 chemistry, the model system needed more  $\text{SO}_4^{2-}$  and  $\text{NO}_3^-$  on the basis of charge balance  
480 and the thermodynamic equilibrium shifted to the direction of consuming Ca Mg, K  
481 and Na, which resulted in the increase of the simulated concentration of  $\text{SO}_4^{2-}$  and  $\text{NO}_3^-$ .  
482 Meanwhile, according to the rule of anions preferentially binding with nonvolatile  
483 cations in ISORROPIA, the increased cations  $\text{Na}^+$ ,  $\text{K}^+$ ,  $\text{Mg}^{2+}$ ,  $\text{Ca}^{2+}$  directly led to  
484 the decrease of anions binding with  $\text{NH}_4^+$ , there were less reaction dose between  $\text{SO}_4^{2-}$   
485 and  $\text{NH}_4^+$  to form  $(\text{NH}_4)_2\text{SO}_4$  or  $\text{NH}_4\text{HSO}_4$ , ultimately resulted in a decrease in  
486 simulated concentration of  $\text{NH}_4^+$  compared with the base case. Because in this case  
487 more anions such as  $\text{SO}_4^{2-}$  were passively needed, according to the principle of chemical  
488 equilibrium mentioned above, the chemical conversion of  $\text{SO}_2$  to  $\text{SO}_4^{2-}$  was promoted,  
489 the simulated secondary  $\text{SO}_4^{2-}$  increased, this could be proved by that the sensitivity  
490 coefficient  $\delta$  of  $\text{SO}_2$  in Case DBP was negative (shown in Fig. 67, details of other  
491 monitoring stations' results were shown Table S24S25).



492

493 Fig.6-7 The sensitivity coefficients ( $\delta$ ) of simulated gas pollutants to the change of adopted source  
494 profile in different cases.



495 Similarly, with the increase of metal ions in the system to bond with anions, the  
496 number of anions which can bind to  $\text{NH}_4^+$  decreased. The system needed less  $\text{NH}_4^+$  and  
497 weakened the need for conversion from  $\text{NH}_3$  to  $\text{NH}_4^+$ , the simulated  $\text{NH}_4^+$  concentration  
498 decreased while the  $\delta$  of  $\text{NH}_3$  was positive and very sensitive. Different trends of  
499 simulated concentration of gaseous pollutants mirrored the rules mentioned above from  
500 another aspect. The  $\delta$  of  $\text{SO}_2$  and  $\text{NO}_x$  was negative,  $\text{NH}_3$  was positive. We could see  
501 the same phenomena in DBL case (Fig. 67). When the percentages of Non-SNA in  
502 source profile increased, they not only affected the simulated concentration of Non-  
503 SNA, but also the secondary  $\text{SO}_4^{2-}$ ,  $\text{NO}_3^-$  and  $\text{NH}_4^+$ .

504 In  $\text{SO}_4^{2-}$  perturbation cases (Case DBS and TPS), as the percentage of  $\text{SO}_4^{2-}$  in  
505 source profile increased, for the chemical reactions of sulfate radical consuming (as  
506 shown in Table S22), the chemical equilibrium would move toward the products  
507 compared with the base case. While for the chemical reactions of sulfate radical  
508 formation (The equations were shown in Table S23), meant the product was added in,  
509 the chemical equilibrium would be pushed toward the reactants. The chemical reactions  
510 between  $\text{SO}_4^{2-}$  and  $\text{NH}_4^+$  would shift to the direction of  $(\text{NH}_4)_2\text{SO}_4$  or  $\text{NH}_4\text{HSO}_4$   
511 generation, we could see the simulated concentrations of  $\text{NH}_4^+$  in DBS and TPS were  
512 both higher and  $\text{NH}_3$  were lower than those in the base case (SGL). In addition, when  
513 more  $\text{SO}_4^{2-}$  was added in the system, the conversion of  $\text{SO}_2$  to  $\text{SO}_4^{2-}$  was affected in  
514 some level and consumed less  $\text{SO}_2$  than the base case, simulated  $\text{SO}_2$  showed insensitive  
515 but positive trend (Fig. 97). And the potential solid phase species in ISORROPIA II  
516 under DBS and TPS cases (shown in Table 2S27) were mainly consisted of sulfate salts,  
517 so the simulated concentration of  $\text{NO}_3^-$  did not change apparently.

518 As the percentage of  $\text{NO}_3^-$  in source profile increased (Case FON and TWN), the  
519 associated chemical equilibrium shifted towards the consumption of  $\text{NO}_3^-$ , such as  $\text{NH}_4^+$   
520 +  $\text{NO}_3^- \rightarrow \text{NH}_4\text{NO}_3$ , which would also consume more  $\text{NH}_4^+$  and form more ammonium  
521 salt, finally consumed more  $\text{NH}_3$  because of  $\text{NH}_3(\text{gas}) + \text{H}_2\text{O}(\text{aq}) \rightarrow \text{NH}_4^+(\text{aq}) + \text{OH}^-$   
522 (aq). The simulation results also manifested that the concentration of  $\text{NH}_4^+$  increased  
523 while that of  $\text{NH}_3$  decreased. Based on the assumption of ISORROPIA, the cations like

524  $\text{Na}^+$ ,  $\text{K}^+$ ,  $\text{Mg}^{2+}$ ,  $\text{Ca}^{2+}$  and  $\text{NH}_4^+$  preferentially to react with  $\text{SO}_4^{2-}$ , only if there were  
525 cations left after neutralized  $\text{SO}_4^{2-}$ , could they react with  $\text{NO}_3^-$  to form salts, so the  
526 simulated concentration of  $\text{SO}_4^{2-}$  was not obviously changed. Accordingly, the  
527 simulated concentration of  $\text{NO}_x$  and  $\text{SO}_2$  almost unchanged (The  $\delta$  of  $\text{NO}_x$  and  $\text{SO}_2$   
528 displayed insensitive).

529 In the cases of  $\text{NH}_4^+$  perturbation (Case OHA and THA), when the percentage of  
530  $\text{NH}_4^+$  in source profile increased, the related chemical equilibrium shifted towards the  
531 direction of  $\text{NH}_4^+$  consumption, such as in  $2\text{NH}_4^+ + \text{SO}_4^{2-} \rightarrow (\text{NH}_4)_2\text{SO}_4$  or  $\text{NH}_4^+ + \text{H}^+$ ,  
532  $\text{SO}_4^{2-} \rightarrow \text{NH}_4\text{HSO}_4$ , more  $\text{SO}_4^{2-}$  was consumed at the same time, which further  
533 promoted the conversion of  $\text{SO}_2$  to  $\text{SO}_4^{2-}$ . The increased  $\text{NH}_4^+$  in OHA and THA also  
534 would inhibit the conversion of  $\text{NH}_3$  to  $\text{NH}_4^+$  compared with the base case. This, in turn  
535 appeared as the increase of the simulated secondary  $\text{SO}_4^{2-}$  and  $\text{NH}_3$ , and the decrease  
536 of the simulated  $\text{SO}_2$ .

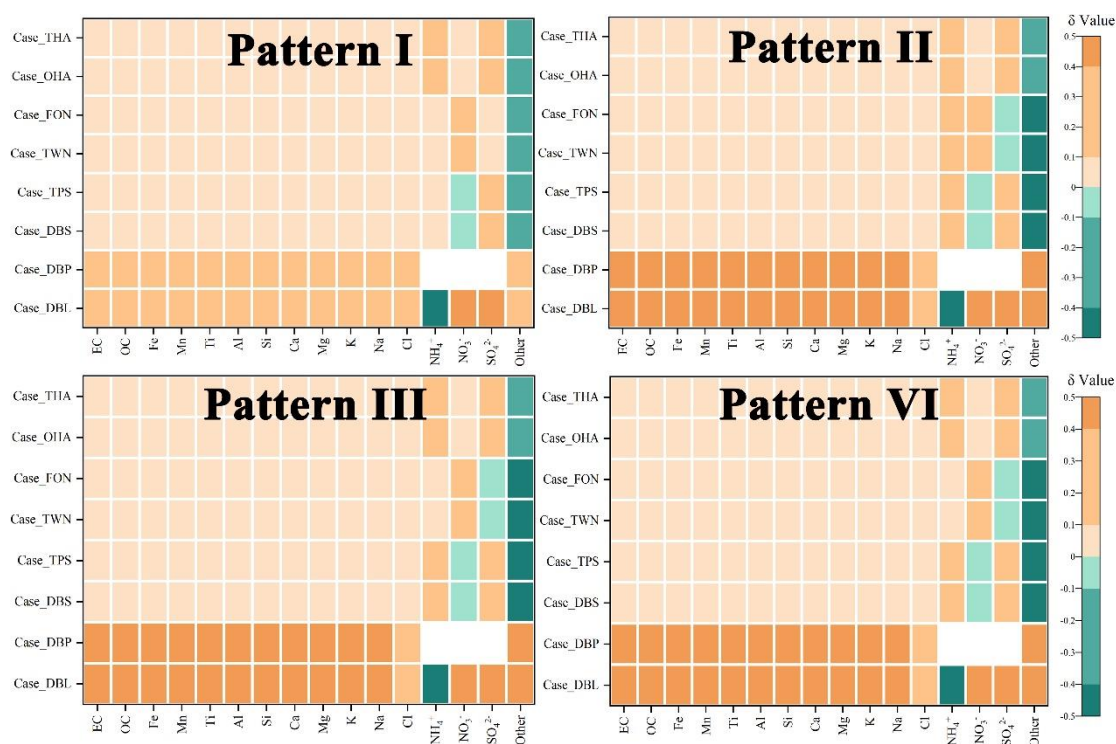
## 537 **5.2 Results from stratified analysis**

538 For each case, the distribution of R values was related to meteorological conditions  
539 (as shown in Fig. 6). To illustrate the role of meteorological conditions in the  
540 mechanism of how source profile affected the simulated  $\text{PM}_{2.5}$  components, stratified  
541 analysis was used. The hourly simulation result of temperature and humidity (affecting  
542 ISORROPIA solving procedure), wind field (affecting flux in and flux out for each grid)  
543 were incorporate into K-means clustering. When the number of clusters was equal to or  
544 greater than 4, there was a significant inflection point between data points and their  
545 assigned cluster centroids (Figure S9). Hence, 4 patterns of meteorological conditions  
546 were selected to the subsequent analysis.

547 For pattern I, II, III and IV, as shown in Fig. 8, the rule similar to the general result  
548 was observed. From a global view, the subdivisional (category-specific) sensitivity of  
549 simulated  $\text{PM}_{2.5}$  components to source chemical profile under different patterns are  
550 similar; From a local perspective, their sensitivity levels are slightly different; For  
551 example, in pattern II, the simulated  $\text{NH}_4^+$  was very sensitive to the perturbation of  
552  $\text{SO}_4^{2-}$ ; While in pattern I, III and VI was sensitive, but it remained the major component

553 that underwent change (These results were also shown in Table S28 of supplementary  
554 material).

555 When we perturb source profile, some species/reactants increase (or reduce) in the  
556 system, the chemical equilibrium shift to the direction of consuming more (or less)  
557 reactants, as shown in Figure S10. Under different patterns of meteorological conditions  
558 (determining the values of R), the influence pathways of chemical source profile  
559 changes on the simulated PM<sub>2.5</sub> components have the same laws with general results.



560

561

Fig. 8 The sensitivity coefficients ( $\delta$ ) under different hierarchical patterns

562 In summary, the effects of source profile variation on the simulation results of  
563 different components were linked. When the percentages of Non-SNA,  $\text{SO}_4^{2-}$ ,  $\text{NO}_3^-$  and  
564  $\text{NH}_4^+$  in the source profile changed, they not only affected the simulated concentration  
565 of themselves, but also affected the simulation results of some other components. Both  
566 the simulation results of primary components and secondary components were affected  
567 by the change of source profile, the secondary  $\text{SO}_4^{2-}$  and  $\text{NH}_4^+$  were affected more than  
568 the secondary  $\text{NO}_3^-$ .

## 569 **6 Conclusions**

570 The influence of source profile variation on the simulated PM<sub>2.5</sub> components  
571 cannot be ignored, as simulation results of some components are sensitive to the  
572 adopted source profile in CTMs, e.g., both the simulated Non-SNA and SNA are  
573 sensitive to the perturbation of Non-SNA in source profile, the simulated SO<sub>4</sub><sup>2-</sup> and  
574 NH<sub>4</sub><sup>+</sup> are sensitive to the perturbation of SO<sub>4</sub><sup>2-</sup>, simulated NO<sub>3</sub><sup>-</sup> and NH<sub>4</sub><sup>+</sup> are sensitive  
575 to the perturbation of NO<sub>3</sub><sup>-</sup>, SO<sub>4</sub><sup>2-</sup> and NH<sub>4</sub><sup>+</sup> are sensitive to the perturbation of NH<sub>4</sub><sup>+</sup>.  
576 These influences are not only specific to an individual component, but also can be  
577 transmitted and linked among components. The influence path is connected to chemical  
578 mechanisms in the model since the variation of species allocation in emission sources  
579 directly affect the thermodynamic equilibrium system (ISORROPIA II, SO<sub>4</sub><sup>2-</sup>-NO<sub>3</sub><sup>-</sup>-Cl<sup>-</sup>  
580 -NH<sub>4</sub><sup>+</sup>-Na<sup>+</sup>-K<sup>+</sup>-Mg<sup>2+</sup>-Ca<sup>2+</sup>-H<sub>2</sub>O system).

581 It is generally believed that changes in source profile would have an impact on the  
582 simulation result of primary PM<sub>2.5</sub>, but interestingly, the simulation of secondary  
583 components could be affected as well. We found the perturbation of PM<sub>2.5</sub> source profile  
584 caused the variation of simulation results of gaseous pollutants by influencing related  
585 chemical reactions like gas-phase chemistry of SO<sub>2</sub>, NO<sub>x</sub> and NH<sub>3</sub>. Overall, the  
586 emission source profile used in CTMs is one of the important factors affecting the  
587 simulation results of PM<sub>2.5</sub> chemical components. Additionally, organic species are one  
588 of the most important components in PM<sub>2.5</sub> and gain much more attention on human  
589 health. While the number of organic species in source profile is relatively scarce which  
590 brings a challenge for simulation test designing, the influence of source profile on the  
591 simulation results of organic species is not taken into account in this study.

592 With the change of fuel and raw materials, the development of production  
593 technology and the innovation of pollution treatment technology in recent years, some  
594 components have changed significantly in source profiles. Given the important role of  
595 air quality simulation in decision making for pollution control and health risk  
596 assessment, the representativeness and timeliness of the source profile should be  
597 considered.

598 Our study tentatively discussed the influence mechanism of PM<sub>2.5</sub> emission source  
599 profiles on the simulation results of components in CTMs. The size distribution, mixing  
600 state, aging and solubility for different aerosol components might have something to do  
601 with source profile, how much the influence of source profile changes on the simulation  
602 of these physical and chemical process, is deserved to do in the future.

### 603 **Data availability**

604 The input datasets for WRF simulation are available at  
605 <https://rda.ucar.edu/datasets/ds351.0/index.html> (The National Center for Atmospheric  
606 Research (NCAR)). The Multi-resolution Emission Inventory for China (MEICv1.3) is  
607 available at [http://meicmodel.org/?page\\_id=135](http://meicmodel.org/?page_id=135). The PM<sub>2.5</sub> emission source profiles  
608 from database of Source Profiles of Air Pollution (SPAP)  
609 (<http://www.nkspap.com:9091/>, Nankai university), SPECIATE database  
610 (<https://www.epa.gov/air-emissions-modeling/speciate>, U.S. Environmental Protection  
611 Agency's (EPA)), Mendeley data repository (<https://doi.org/10.17632/x8dfshjt9j.2>, Bi  
612 et al., 2019). [Tutorial guide for accessing Database of Source Profiles of Air Pollution  
613 \(SPAP\), input and output data repository \(<https://zenodo.org/record/7865675>\).](#)

### 614 **Code availability**

615 The source code for CMAQ version 5.0.2 is available at  
616 <https://github.com/USEPA/CMAQ/tree/5.0.2> (last access: April 2014)  
617 (<https://doi.org/10.5281/zenodo.1079898>, US EPA Office of Research and  
618 Development, 2018). The source code for WRF version 3.7.1 is available at  
619 <https://www2.mmm.ucar.edu/wrf/src/WRFV3.7.1.TAR.gz>.

### 620 **Author contributions**

621 Zhongwei Luo: Data curation and collection, writing—original draft. Yan Han:  
622 Modeling, writing—original draft. Kun Hua: Data collection. Yufen Zhang:  
623 Supervision—Review & editing. Jianhui Wu: Supervision in source profile. Xiaohui Bi:  
624 Supervision in source profile. Qili Dai: Resources. Baoshuang Liu: Resources. Yang

625 Chen: Modification and editing. Xin Long: Supervision in modeling. Yinchang Feng:  
626 Supervision–Review & editing.

### 627 **Competing interests**

628 The authors declare that they have no known competing financial interests or  
629 personal relationships that could have appeared to influence the work reported in this  
630 paper.

### 631 **Disclaimer. Publisher’s note**

632 Copernicus Publications remains neutral with regard to jurisdictional claims in  
633 published maps and institutional affiliations.

### 634 **Acknowledgements**

635 We would like to thank the National Natural Science Foundation of China (grant  
636 number 42177465) for providing funding for the project. We are grateful for the  
637 Inventory Spatial Allocate Tool (ISAT) provided by Kun Wang from Department of Air  
638 Pollution Control, Institute of Urban Safety and Environmental Science, Beijing  
639 Academy of Science and Technology. We thank ~~two~~three anonymous referees, Astrid  
640 Kerkweg (Executive Editor) and Klaus Klingmüller (Top Editor) for the time and effort  
641 spent in reviewing the manuscript.

### 642 **Financial support**

643 This study was financially supported by the National Natural Science Foundation  
644 of China (grant number 42177465).

### 645 **Reference**

- 646 Appel, K. W., Poullo, G. A., Simon, H., Sarwar, G., Pye, H. O. T., Napelenok, S. L., Akhtar, F., Roselle,  
647 S. J.: Evaluation of dust and trace metal estimates from the Community Multiscale Air Quality  
648 (CMAQ) model version 5.0, *Geosci. Model Dev.*, 6, 883-899, [https://doi.org/10.5194/gmd-6-883-](https://doi.org/10.5194/gmd-6-883-2013)  
649 [2013](https://doi.org/10.5194/gmd-6-883-2013), 2013.
- 650 Bi, X., Dai, Q., Wu, J., Zhang, Q., Zhang, W., Luo, R., Cheng, Y., Zhang, J., Wang, L., Yu, Z., Zhang, Y.,  
651 Tian, Y., Feng, Y.: Characteristics of the main primary source profiles of particulate matter across  
652 China from 1987 to 2017, *Atmos. Chem. Phys.*, 19, 3223-3243, <https://doi.org/10.5194/acp-19->

653 [3223-2019](#), 2019.

654 Cao, J., Qiu, X., Gao, J., Wang, F., Wang, J., Wu, J., Peng, L.: Significant decrease in SO<sub>2</sub> emission and  
655 enhanced atmospheric oxidation trigger changes in sulfate formation pathways in China during  
656 2008–2016, *J. Clean. Prod.*, 326, 129396, <https://doi.org/10.1016/j.jclepro.2021.129396>, 2021.

657 Chapel Hill, N.: Operational Guidance for the Community Multiscale Air Quality (CMAQ) Mo  
658 deling System Version 5.0, [https://www.airqualitymodeling.org/index.php/CMAQ\\_version\\_5.0](https://www.airqualitymodeling.org/index.php/CMAQ_version_5.0)  
659 [\(February 2010 release\) OGD#Aerosol Module](#), last access: February 2012.

660 Chen, Z., Chen, D., Zhao, C., Kwan, M., Cai, J., Zhuang, Y., Zhao, B., Wang, X., Chen, B., Yang, J., Li,  
661 R., He, B., Gao, B., Wang, K., Xu, B.: Influence of meteorological conditions on PM<sub>2.5</sub>  
662 concentrations across China: A review of methodology and mechanism, *Environ. Int.*, 139, 105558,  
663 <https://doi.org/10.1016/j.envint.2020.105558>, 2020.

664 Cheng, N. L., Meng, F., Wang, J. K., Chen, Y. B., Wei, X., Han, H.: Numerical simulation of the spatial  
665 distribution and deposition of PM<sub>2.5</sub> in East China coastal area in 2010 (In Chinese), *Journ. Safety*  
666 *Environ.*, 15, 305-310, <https://doi.org/10.13637/j.issn.1009-6094.2015.06.063>, 2015.

667 Eder, B. K., Yu, S. C.: A performance evaluation of the 2004 release of Models-3 CMAQ, *Atmos.*  
668 *Environ.*, 40, 4811-4824, [http://doi.org/10.1007/978-0-387-68854-1\\_57](http://doi.org/10.1007/978-0-387-68854-1_57), 2006.

669 Foley, K. M., Roselle, S. J., Appel, K. W., Bhawe, P. V., Pleim, J., Otte, T., Mathur, R., Sarwar, G., Young,  
670 J. O., Gilliam, R.: Incremental testing of the community multiscale air quality (CMAQ) modeling  
671 system version 4.7, *Geosci. Model Dev.*, 3, 205-226, <https://doi.org/10.5194/gmd-3-205-2010>, 2010.

672 Fountoukis, C., Nenes, A.: ISORROPIA II: a computationally efficient thermodynamic equilibrium  
673 model for K<sup>+</sup>-Ca<sup>2+</sup>-Mg<sup>2+</sup>-NH<sub>4</sub><sup>+</sup>-Na<sup>+</sup>-SO<sub>4</sub><sup>2-</sup>-NO<sub>3</sub><sup>-</sup>-Cl<sup>-</sup>-H<sub>2</sub>O aerosols, *Atmos. Chem. Phys.*, 7,  
674 4639-4659, <https://doi.org/10.5194/acp-7-4639-2007>, 2007.

675 Fu, X., Wang, S., Zhao, B., Xing, J., Cheng, Z., Liu, H., Hao, J.: Emission inventory of primary pollutants  
676 and chemical speciation in 2010 for the Yangtze River Delta region, China, *Atmos. Environ.*, 70,  
677 39-50, <https://doi.org/10.1016/j.atmosenv.2012.12.034>, 2013.

678 Fu, X., Wang, S. X., Chang, X., Cai, S., Xing, J., Hao, J. M.: Modeling analysis of secondary inorganic  
679 aerosols over China: pollution characteristics, and meteorological and dust impacts, *Sci. Rep.*, 6,  
680 35992, <https://doi.org/10.1038/srep35992>, 2016.

681 Gao, S., Zhang, S., Che, X., Ma, Y., Chen, X., Duan, Y., Fu, Q., Wang, S., Zhou, B., Wei, C., Jiao, Z.:  
682 New understanding of source profiles: Example of the coating industry, *J. Clean. Prod.*, 357, 132025,  
683 <https://doi.org/10.1016/j.jclepro.2022.132025>, 2022.

684 Guo, R., Yang, J., Liu, Z.: Influence of heat treatment conditions on release of chlorine from Datong coal,  
685 *J. Anal. Appl. Pyrol.*, 71, 179-186, [https://doi.org/10.1016/S0165-2370\(03\)00086-X](https://doi.org/10.1016/S0165-2370(03)00086-X), 2004.

686 Guo, Y. Y., Gao, X., Zhu, T. Y., Luo, L., Zheng, Y.: Chemical profiles of PM emitted from the iron and  
687 steel industry in northern China, *Atmos. Environ.*, 150, 187-197,  
688 <https://doi.org/10.1016/j.atmosenv.2016.11.055>, 2017.

689 Guo, Z., Hao, Y., Tian, H., Bai, X., Wu, B., Liu, S., Luo, L., Liu, W., Zhao, S., Lin, S., Lv, Y., Yang, J.,  
690 Xiao, Y.: Field measurements on emission characteristics, chemical profiles, and emission factors  
691 of size-segregated PM from cement plants in China, *Sci. Total Environ.*, 151822,  
692 <https://doi.org/10.1016/j.scitotenv.2021.151822>, 2021.

693 Han, Y., Xu, H., Bi, X. H., Lin, F. M., Li, J., Zhang, Y. F., Feng, Y. C.: The effect of atmospheric  
694 particulates on the rainwater chemistry in the Yangtze River Delta, China, *J. Air Waste Manage.*, 69,  
695 1452-1466, <https://doi.org/10.1080/10962247.2019.1674750>, 2019.

696 Hopke, P. K., Dai, Q., Li, L., Feng, Y.: Global review of recent source apportionments for airborne



697 particulate matter, *Sci. Total Environ.*, 740, 140091,  
698 <https://doi.org/10.1016/j.scitotenv.2020.140091>, 2020.

699 Hopke, P. K., Feng, Y. C., Dai, Q.: Source apportionment of particle number concentrations: A global  
700 review, *Sci. Total Environ.*, 819, 153104, <https://doi.org/10.1016/j.scitotenv.2022.153104>, 2022.

701 Hsu, Y., Divita, F., Dorn, J.: SPECIATE 5.0 - Speciation Database Development Documentation, Final  
702 Report, M. MENETREZ, Abt Associates Inc./Office of Research and Development/U.S.  
703 Environmental Protection Agency Research Triangle Park, NC27711,  
704 [https://www.epa.gov/sites/default/files/2019-07/documents/speciate\\_5.0.pdf](https://www.epa.gov/sites/default/files/2019-07/documents/speciate_5.0.pdf), 2019.

705 Huang, C. H., Hu, J. L., Xue, T., Xu, H., Wang, M.: High-Resolution Spatiotemporal Modeling for  
706 Ambient PM<sub>2.5</sub> Exposure Assessment in China from 2013 to 2019, *Environ. Sci. Technol.*, 55, 2152-  
707 2162, <https://doi.org/10.1021/acs.est.0c05815>, 2021.

708 Huang, Z. J., Zheng, J. Y., Qu, J. M., Zhong, Z. M., Wu, Y. Q., Shao, M.: A Feasible Methodological  
709 Framework for Uncertainty Analysis and Diagnosis of Atmospheric Chemical Transport Models,  
710 *Environ. Sci. Technol.*, 53, 3110-3118, <https://doi.org/10.1021/acs.est.8b06326>, 2019.

711 Ji, Z., Gan, M., Fan, X., Chen, X., Li, Q., Lv, W., Tian, Y., Zhou, Y., Jiang, T.: Characteristics of PM<sub>2.5</sub>  
712 from iron ore sintering process: Influences of raw materials and controlling methods, *J. Clean. Prod.*,  
713 148, 12-22, <https://doi.org/10.1016/j.jclepro.2017.01.103>, 2017.

714 Li, J., Wu, Y., Ren, L., Wang, W., Tao, J., Gao, Y., Li, G., Yang, X., Han, Z., Zhang, R.: Variation in PM<sub>2.5</sub>  
715 sources in central North China Plain during 2017–2019: Response to mitigation strategies, *J.*  
716 *Environ. Manage.*, 28, 112370, <https://doi.org/10.1016/j.jenvman.2021.112370>, 2021.

717 Li, M., Hu, M., Du, B., Guo, Q., Tan, T., Zheng, J., Huang, X., He, L., Wu, Z., Guo, S.: Temporal and  
718 spatial distribution of PM<sub>2.5</sub> chemical composition in a coastal city of Southeast China, *Sci. Total*  
719 *Environ.*, 605-606, 337-346, <https://doi.org/10.1016/j.scitotenv.2017.03.260>, 2017a.

720 Li, M., Liu, H., Geng, G., Hong, C., Liu, F., Song, Y., Tong, D., Zheng, B., Cui, H., Man, H., Zhang, Q.,  
721 He, K.: Anthropogenic emission inventories in China: a review, *Natl. Sci. Rev.*, 4, 834-866,  
722 <https://doi.org/10.1093/nsr/nwy044>, 2017b.

723 Li, X., He, K., Li, C., Yang, F., Zhao, Q., Ma, Y., Chen, Y., Ouyang, W., Chen, G.: PM<sub>2.5</sub> mass, chemical  
724 composition, and light extinction before and during the 2008 Beijing Olympics, *J. Geophys. Res.*,  
725 118, 12158-12167, <https://doi.org/10.1002/2013JD020106>, 2013.

726 Liang, F., Xiao, Q., Yang, X., Liu, F., Li, J., Lu, X., Liu, Y., Gu, D.: The 17-y spatiotemporal trend of  
727 PM<sub>2.5</sub> and its mortality burden in China, *Proc. Natl. Acad. Sci.*, 117, 25601-25608,  
728 <https://doi.org/10.1073/pnas.1919641117>, 2020.

729 Lv, L., Wei, P., Li, J., Hu, J.: Application of machine learning algorithms to improve numerical simulation  
730 prediction of PM<sub>2.5</sub> and chemical components, *Atmos. Pollut. Res.*, 12, 101211,  
731 10.1016/j.apr.2021.101211, 2021.

732 NBS (National Bureau of Statistics of China): China Statistical Yearbook 2021,  
733 <http://www.stats.gov.cn/tjsj/ndsj/2021/indexch.htm>, last access: 2022.

734 Peterson, G., Hogrefe, C., Corrigan, A., Neas, L., Mathur, R., Rappold, A.: Impact of Reductions in  
735 Emissions from Major Source Sectors on Fine Particulate Matter–Related Cardiovascular Mortality,  
736 *Environ. Health Persp.*, 128, 017005, <https://doi.org/10.1289/EHP5692>, 2020.

737 Qi, H., Cui, C., Zhao, T., Bai, Y., Liu, L.: Numerical simulation on the characteristics of PM<sub>2.5</sub> heavy  
738 pollution and the influence of weather system in Hubei Province in winter 2015 (In Chinese),  
739 *Meteorological monthly*, 45, 1113-1122, <https://doi.org/10.7519/j.issn.1000-0526.2019.08.008>,  
740 2019.



741 Seinfeld, J. H., Pandis, S. N.: Atmospheric Chemistry and Physics, from air pollution to climate change.  
742 John Wiley & Sons, Inc., Hoboken, New Jersey.47-61, ISBN9781119221166, 2006

743 Sha, T., Ma, X., Jia, H., Tian, R., Chang, Y., Cao, F., Zhang, Y.: Aerosol chemical component: Simulations  
744 with WRF-Chem and comparison with observations in Nanjing, Atmos. Environ., 218, 1-14,  
745 <https://doi.org/10.1016/j.atmosenv.2019.116982>, 2019.

746 Shi, W., Liu, C., Norback, D., Deng, Q., Huang, C., Qian, H., Zhang, X., Sundell, J., Zhang, Y., Li, B.,  
747 Kan, H., Zhao, Z.: Effects of fine particulate matter and its constituents on childhood pneumonia: a  
748 cross-sectional study in six Chinese cities, Lancet, 392, S79, [https://doi.org/10.1016/S0140-](https://doi.org/10.1016/S0140-6736(18)32708-9)  
749 [6736\(18\)32708-9](https://doi.org/10.1016/S0140-6736(18)32708-9), 2018.

750 Shi, Z., Li, J., Huang, L., Wang, P., Wu, L., Ying, Q., Zhang, H., Lu, L., Liu, X., Liao, H., Hu, J.: Source  
751 apportionment of fine particulate matter in China in 2013 using a source-oriented chemical transport  
752 model, Sci. Total Environ., 601-602, 1476-1487, <https://doi.org/10.1016/j.scitotenv.2017.06.019>,  
753 2017.

754 Song, S. Y., Wang, Y. S., Wang, Y. L., Wang, T., Tan, H. Z.: The characteristics of particulate matter and  
755 optical properties of Brown carbon in air lean condition related to residential coal combustion,  
756 Powder Technol., 379, 505-514, <https://doi.org/10.1016/j.powtec.2020.10.082>, 2021.

757 Tang, X. Y., Zhang, Y. H., Shao, M.: Atmosphere Environment Chemistry, Second ed (In Chinese). .  
758 Higher Education Press, Beijing, China.268-329, ISBN978-7-04-019361-9, 2006

759 Wang, C., Zheng, J., Du, J., Wang, G., Klemes, J., Wang, B., Liao, Q., Liang, Y.: Weather condition-  
760 based hybrid models for multiple air pollutants forecasting and minimisation, J. Clean. Prod., 352,  
761 131610, <https://doi.org/10.1016/j.jclepro.2022.131610>, 2022.

762 Wang, D., Hu, J., Xu, Y., Lv, D., Xie, X., Kleeman, M., Xing, J., Zhang, H., Ying, Q.: Source  
763 contributions to primary and secondary inorganic particulate matter during a severe wintertime  
764 PM<sub>2.5</sub> pollution episode in Xi'an, China, Atmos. Environ., 97, 182-194,  
765 <https://doi.org/10.1016/j.atmosenv.2014.08.020>, 2014.

766 Weagle, C., Sinder, G., Li, C. C., Donkelaar, A., S, P., Bissonnette, P., Burke, I., Jackson, J., Latimer, R.,  
767 Stone, E., Abboud, I., Akoshile, C., Anh, N., Brook, J., Cohen, A., Dong, J., Gibson, M., Griffith,  
768 D., He, K., Holben, B., Kahn, R., Keller, C., Kim, J., Lagrosas, N., Lestari, P., Khian, Y., Liu, Y.,  
769 Marais, E., Martins, J., Misra, A., Muliane, U., Pratiwi, R., Quel, E., Salam, A., Segey, L., Tripathi,  
770 S., Wang, C., Zhang, Q., Brauer, M., Rudich, Y., Martin, R.: Global Sources of Fine Particulate  
771 Matter: Interpretation of PM<sub>2.5</sub> Chemical Composition Observed by SPARTAN using a Global  
772 Chemical Transport Model, Environ. Sci. Technol., 52, 11670-11681,  
773 <https://doi.org/10.1021/acs.est.8b01658>, 2018.

774 Wongphatarakul, V., Friedlander, S. K., Pinto, J. P.: A Comparative Study of PM<sub>2.5</sub> Ambient Aerosol  
775 Chemical Databases, Environ. Sci. Technol., 32, 3926-3934, <https://doi.org/10.1021/es9800582>,  
776 1998.

777 Wu, B., Bai, X., Liu, W., Zhu, C., Hao, Y., Lin, S., Liu, S., Luo, L., Liu, X., Zhao, S., Hao, J., Tian, H.:  
778 Variation characteristics of final size-segregated PM emissions from ultralow emission coal-fired  
779 power plants in China, Environ. Pollut., 259, 113886, <https://doi.org/10.1016/j.envpol.2019.113886>,  
780 2020.

781 Wu, D., Zheng, H., Li, Q., Jin, L., Lyu, R., Ding, X., Huo, Y., Zhao, B., Jiang, J., Chen, J., Li, X., Wang,  
782 S.: Toxic potency-adjusted control of air pollution for solid fuel combustion, Nat. Energy, 7, 194-  
783 202, <https://doi.org/10.1038/s41560-021-00951-1>, 2022.

784 Wu, Z. X., Hu, T. F., Hu, W., Shao, L. Y., Sun, Y. Z., Xue, F. L., Niu, H. Y.: Evolution in physicochemical

785 properties of fine particles emitted from residential coal combustion based on chamber experiment,  
786 Gondwana Res., <https://doi.org/10.1016/j.gr.2021.10.017>, 2021.

787 Xia, Z. Q., Fan, X. L., Huang, Z. J., Liu, Y. C., Yin, X. H., Ye, X., Zheng, J. Y.: Comparison of Domestic  
788 and Foreign PM<sub>2.5</sub> Source Profiles and Influence on Air Quality Simulation (In Chinese), Res.  
789 Environ. Sci., 30, 359-367, <https://doi.org/10.13198/j.issn.1001-6929.2017.01.55>, 2017.

790 Yang, F., Tan, J., Zhao, Q., Du, Z., He, K., Ma, Y., Duan, F., Chen, G., Zhao, Q.: Characteristics of PM<sub>2.5</sub>  
791 speciation in representative megacities and across China, Atmos. Chem. Phys., 11, 1025-1051,  
792 <https://doi.org/10.5194/acpd-11-1025-2011>, 2011.

793 Ying, Q., Feng, M., Song, D. L., Wu, L., Hu, J., Zhang, H., Kleeman, M., Li, X.: Improve regional  
794 distribution and source apportionment of PM<sub>2.5</sub> trace elements in China using inventory-observation  
795 constrained emission factors, Sci. Total Environ., 624, 355-365,  
796 <https://doi.org/10.1016/j.scitotenv.2017.12.138>, 2018.

797 Yu, S. C., Mathur, R., Pleim, J., Wong, D., Gilliam, R., Alapaty, K., Zhao, C., Liu, X.: Aerosol indirect  
798 effect on the grid-scale clouds in the two-way coupled WRF-CMAQ: model description,  
799 development, evaluation and regional analysis, Atmos. Chem. Phys., 14, 11247-11285,  
800 <http://10.5194/acp-14-11247-2014>, 2014.

801 Yu, Z. C., Jang, M., Kim, S., Bae, C., Koo, B., Beardsley, R., Park, J., Chang, L., Lee, H., Lim, Y., Cho,  
802 J.: Simulating the Impact of Long-Range-Transported Asian Mineral Dust on the Formation of  
803 Sulfate and Nitrate during the KORUS-AQ Campaign, Earth Space Chem., 4, 1039-1049,  
804 <https://doi.org/10.1021/acsearthspacechem.0c00074>, 2020.

805 Zhang, J., Wu, J., Lv, R., Song, D., Huang, F., Zhang, Y., Feng, Y.: Influence of Typical Desulfurization  
806 Process on Flue Gas Particulate Matter of Coal-fired Boilers (In Chinese), Environ. Sci., 41, 4455-  
807 4461, <https://doi.org/10.13227/j.hjcx.202003193>, 2020.

808 Zhang, Q., Xue, D., Wang, S., Wang, L., Wang, J., Ma, Y., Liu, X.: Analysis on the evolution of PM<sub>2.5</sub>  
809 heavy air pollution process in Qingdao (In Chinese), China Environ. Sci., 37, 3623-3635,  
810 <https://doi.org/10.3969/j.issn.1000-6923.2017.10.003>, 2017.

811 Zhang, S. P., Xing, J., Sarwar, G., Ge, Y. L., He, H., Duan, F., Zhao, Y., He, K., Zhu, L., Chu, B.:  
812 Parameterization of heterogeneous reaction of SO<sub>2</sub> to sulfate on dust with coexistence of NH<sub>3</sub> and  
813 NO<sub>2</sub> under different humidity conditions, Atmos. Environ., 208, 133-140,  
814 <https://doi.org/10.1016/j.atmosenv.2019.04.004>, 2019.

815 Zheng, B., Tong, D., Li, M., Liu, F., Hong, C., Geng, G., Li, H., Li, X., Peng, L., Qi, J., Yan, L., Zhang,  
816 Y., Zhao, H., Zheng, Y., He, K., Zhang, Q.: Trends in China's anthropogenic emissions since 2010  
817 as the consequence of clean air actions, Atmos. Chem. Phys., 18, 14095-14111,  
818 <https://doi.org/10.5194/acp-18-14095-2018>, 2018.

819 Zheng, B., Zhang, Q., Zhang, Y., He, K. B., Wang, K., Zheng, G. J., Duan, F. K., Ma, Y. L., Kimoto, T.:  
820 Heterogeneous chemistry: a mechanism missing in current models to explain secondary inorganic  
821 aerosol formation during the January 2013 haze episode in North China, Atmos. Chem. Phys., 15,  
822 2031-2049, [10.5194/acp-15-2031-2015](https://doi.org/10.5194/acp-15-2031-2015), 2015.

823 Zheng, H., Song, S., Sarwar, G., Gen, M., Wang, S., Ding, D., Chang, X., Zhang, S., Xing, J., Sun, Y. L.,  
824 Ji, D., Chan, C. K., Gao, J., McElroy, M.: Contribution of Particulate Nitrate Photolysis to  
825 Heterogeneous Sulfate Formation for Winter Haze in China, Environ. Sci. Technol. Lett., 7, 632-  
826 638, <https://doi.org/10.1021/acs.estlett.0c00368>, 2020.

827 Zhou, L., Chen, X., Tian, X.: The impact of fine particulate matter (PM<sub>2.5</sub>) on China's agricultural  
828 production from 2001 to 2010, J. Clean. Prod., 178, 133-141,

829 <https://doi.org/10.1016/j.jclepro.2017.12.204>, 2018.

830